

Master's thesis

Master's degree in automatic control and robotics (MUAR)

Construction and control of a magnetic levitation system

Author: María Mercadé de Luna

Director: Manel Velasco

Deadline: April 2023



Escola Tècnica Superior
d'Enginyeria Industrial de Barcelona

ETSEIB

The word "ETSEIB" is displayed in large, bold, light blue capital letters. A smaller, darker blue circular logo containing a grid of dots and the letters "UPC" is positioned between the "T" and the "S".

Abstract

This project aimed to design and build a low-cost magnetic levitation system based on attraction, using a single coil. The materials and components were carefully selected to keep the cost of the system as low as possible, making it suitable for educational purposes such as laboratory demonstrations or science classes.

The system consists of a base made of aluminium and PLA onto which a single coil has been screwed. The intention of the project is to levitate a neodymium magnet underneath the coil by constructing a levitator that works by attraction, i.e. that compensates the force of gravity that the magnet suffers to keep the magnet floating in the air. A PID control algorithm has been implemented using an Arduino microcontroller to regulate the levitation distance between the magnet and the coil.

The design and construction of the system were performed with an emphasis on simplicity and affordability. The use of a single coil and inexpensive materials made it possible to achieve a functional prototype at a low cost. The system was tested and the performance of the PID controller was evaluated.

The results showed that the system was able to achieve stable magnetic levitation. However, the tuning of the PID parameters was found to be challenging due to the non-linear behavior of the system and an unexpected behavior of the sensor that was expected to give measurements of the magnet position. The sensitivity of the system to external disturbances and noise was also observed.

Therefore, a low-cost attraction-based magnetic levitation system was successfully designed and implemented using a single coil, a hall effect sensor and an Arduino microcontroller with a PID control algorithm. The system provides a valuable educational tool for teaching principles of electromagnetics and control engineering. Future work could focus on further improving the system's performance through the use of more advanced control strategies, such as a sliding mode or fuzzy-logic control.

Contents

1	Introduction	6
1.1	Project Objectives	6
1.2	Project Scope	6
2	Theoretical Background	8
2.1	History and Discovery of Electromagnetism	8
2.2	State of the art: existing magnetic levitation applications	9
2.2.1	Maglev for transportation	9
2.2.2	Maglev in microrobotics	11
2.2.3	Maglev in healthcare	11
2.2.4	Maglev in magnetic bearings	12
2.2.5	Maglev in education	12
2.3	Existing low-cost magnetic levitation systems	13
3	Design and construction of the magnetic levitation prototype	16
3.1	Fabrication of the structure	17
3.2	Arduino Uno	19
3.3	Hall-effect sensor	20
3.4	Levitator electromagnet	21
3.5	Arduino motorshield	21
3.6	Complete system	23
4	Dynamic modeling of the Magnetic Levitation System	24
4.1	Dynamic equations of the system	24
4.1.1	Mechanical part	25
4.1.2	Electrical part	25
4.2	State space representation of the system	26
4.3	Linearization of the system	27
4.4	Parameter Estimation	28
4.5	Transfer function analysis	29
5	System control through a PID	32
5.1	PID control theory	32
5.2	PID simulation	33
5.2.1	Simulation of the plant without controller	36
5.2.2	Simulation of the closed loop system with PD	37
5.3	Implementation of the controller and real-time system operation	38

5.3.1	Sensor calibration	38
5.3.2	PID controller	39
6	Project planning	43
6.1	Gantt chart	43
7	Project related costs	45
7.1	Cost of the prototype	45
7.2	Electricity costs	46
8	Project impact	47
8.1	Environmental impact	47
8.2	Impact on gender equality	48
	Conclusions: discussion of limitations and future improvements	49
	Acknowledgments	50
	Bibliography	51
	Annexes	54

List of Figures

2.1	Japanese superconducting maglev system L0 expected to be in service in 2027 [4]	10
2.2	Magnetic bearing [9]	12
2.3	Magnetic levitator prototype from [10]	13
2.4	Magnetic levitator prototype from [11]	14
2.5	Magnetic levitator prototype from [12]	14
2.6	Magnetic levitator prototype from [13]	15
3.1	Solidworks design of the levitator prototype	17
3.2	Arduino container box being 3D printed	18
3.3	Constructed structure	19
3.4	Arduino board [15]	19
3.5	Hall effect sensor pinout [16]	20
3.6	Heschen electromagnet [17]	21
3.7	Arduino motorshield Rev3 [18]	22
3.8	Assembled and working levitator	23
4.1	Model of the magnetic levitation system [20]	24
5.1	Root locus of the system with P controller	34
5.2	Detail of the root locus with P controller	34
5.3	Root locus of the system with Kp and Kd	35
5.4	Detail of the root locus with Kp and Kd	35
5.5	Open-loop system Simulink scheme	36
5.6	System output for z initial condition bigger than z^*	36
5.7	System output for z initial condition lower than z^*	37
5.8	Closed loop system scheme to simulate the behavior with a PD controller	37
5.9	Response of the simulated system with a PD controller	38
5.10	Sensor static calibration	39
5.11	Cancelling out the coil effect on the Hall effect sensor dynamic	40
5.12	Response of the system with a P controller	40
5.13	Response of the system with a PD controller	41
5.14	Response of the system with a PID controller	41
5.15	Response of the system with an integrated PD controller	42
6.1	Gantt diagram of the project	44

Chapter 1

Introduction

The following chapter introduces a project on magnetic levitation, including its objectives and scope, as well as the motivation behind its development.

1.1 Project Objectives

The primary objective of this project is to develop a functional prototype of a magnetic levitation system that can levitate a magnet in a stable manner using different control methods. More specifically, this has resulted in the following objectives:

- Design a functional magnetic levitation prototype that can stably levitate a magnet. A structure to mount and assemble the necessary hardware components will be needed. The system will consist of a controller, a power stage to drive an electromagnet, the electromagnet and some type of sensor that can provide position feedback of the levitating magnet.
- Design and implement a PID controller to regulate the position of the levitated magnet. The controller will be tuned to optimize the system's stability.
- Identify areas for improvement in the magnetic levitation system based on the performance analysis.

1.2 Project Scope

The scope of this project is to design, build and evaluate the performance of a magnetic levitation system that can stably levitate a magnet using control theory. The project will involve the manufacturing of a functional prototype consisting of an Arduino board, an electromagnet, a sensor to provide position feedback and a power stage to drive the electromagnet.

The project aims to implement a control loop for the levitator system. The idea is to optimize its stability. Furthermore, the limitations of the system are going to be identified and further improvements to enhance its performance will be proposed. These improvements may include optimizing the system's hardware or implementing more advanced control techniques.

Overall, this project aims to provide insights into the design and control of magnetic levitation systems.

Chapter 2

Theoretical Background

This chapter introduces readers to the science of magnetic levitation. The chapter starts with an overview of the historical development of electromagnetic theory, laying the groundwork for understanding the principles of magnetic levitation. The next section focuses on the current state of the art in magnetic levitation applications. This section covers various real-world applications of magnetic levitation. Finally, the chapter explores the existing low-cost magnetic levitation prototypes available in the market for educational purposes. This section provides a useful foundation and serves as a guide for the project's levitator design and development process.

2.1 History and Discovery of Electromagnetism

Electromagnetism discovery and understanding have been crucial to the development of physics and technology. Below is a brief history of electromagnetism, which dates back to the early experiments of the 18th century and continues to the modern advances in theory and practical application.

The study of electromagnetism began in earnest in the 18th century when scientists started to investigate the properties of electricity and magnetism independently. The French physicist Charles-Augustin de Coulomb was one of the first to conduct rigorous experiments on electrical and magnetic forces, establishing the fundamental laws of electrostatics and magnetostatics in the 1780s. As the theory developed, it was discovered that the two forces were closely related, leading scientists to investigate the possibility that electricity could produce magnetism and vice versa[1].

In 1820, the Danish physicist Hans Christian Oersted carried out a crucial experiment that demonstrated the connection between electricity and magnetism. Oersted noticed that a nearby compass needle was deflected from its normal position when an electric current was passed through a wire, indicating the presence of a magnetic field generated by the current. This discovery laid the groundwork for the theory of electromagnetism[2].

In 1821 André-Marie Ampère made a significant contribution to the field of electromagnetism. He formulated Ampere's law, which describes the relationship between the current flowing through a conductor and the magnetic field produced by that current. Ampere's work laid the

foundation for the development of the telegraph and other electrical communication systems[3].

The connection between electricity and magnetism was further explored by the British physicist Michael Faraday in the 1830s. Faraday demonstrated that a changing magnetic field could produce an electric current in a circuit, a process known as electromagnetic induction. This discovery led to the creation of the first electric generator, which converts mechanical energy into electrical energy by rotating a magnet inside a coil of wire[1].

The work of Faraday and Oersted laid the foundation for the theory of electromagnetism, which was further developed by the Scottish physicist James Clerk Maxwell in the 1860s. Maxwell formulated a series of mathematical equations that described the interaction of electric and magnetic fields and showed that electromagnetic waves could propagate through empty space at the speed of light. This discovery was crucial to the understanding of light as a form of electromagnetic radiation and led to the unification of electric and magnetic theories into a single theory of electromagnetism[2]. Moreover, this led to another significant milestone which was the foundation for the development of radio communication and other wireless technologies[1].

Overall, the discoveries and developments in electromagnetism during the 19th century revolutionized the world and paved the way for the development of modern technology. The applications of electromagnetism today are vast and varied, including power generation and transmission, telecommunications, medical equipment and many more.

In conclusion, the contributions of many scientists over several decades have led to significant technological advancements that are enjoyed today. The journey began with the initial discovery of the relationship between electricity and magnetism, which opened up new avenues for exploration. Subsequent research and experimentation by scientists such as Faraday, Ampere and Maxwell further advanced the understanding of electromagnetism, culminating in the unification of these two fields.

2.2 State of the art: existing magnetic levitation applications

Magnetic levitation, also known as maglev, is a technology that uses magnetic fields to levitate objects and transport them without physical contact. This concept has been around for over a century, but it wasn't until the 1970s that it was successfully applied to transportation systems. The basic principle of magnetic levitation is to create a repulsive force between two objects with the same polarity in order to overcome the force of gravity, allowing objects to float in mid-air. This force can be created by using permanent magnets or by using electromagnets that can be switched on and off.

Magnetic levitation technology has been applied in various fields such as transportation, robotics and even in the medical industry. In the following subsections, several current applications of magnetic levitation will be discussed in more detail. Each of these applications takes advantage of the unique properties of magnetic levitation to achieve their specific goals.

2.2.1 Maglev for transportation

Maglev technology has shown great promise in the field of transportation, offering advantages such as high speed, low noise and reduced maintenance costs. This technology utilizes magnetic fields to levitate and propel vehicles without the need for physical contact between the vehicle

and the guideway. The principle behind it is the use of superconducting magnets to generate a magnetic field that repels the magnets on the vehicle, lifting it up and allowing it to glide smoothly along the guideway[4].

The concept of maglev transportation has been around for many years, with early experiments dating back to the 1930s. However, it was not until the 1970s that maglev technology began to be developed, with the first commercial maglev system opening in Birmingham, UK, in 1984. Since then, several countries have developed and implemented maglev transportation systems, including Japan, Germany and China. These systems have demonstrated the potential for maglev technology to revolutionize transportation, offering high speeds and reduced environmental impact compared to traditional transportation systems[5].

One of the key advantages of maglev in transportation is its ability to operate at high speeds with minimal noise. Maglev trains are expected to travel at speeds of up to 600 km/h, reducing travel time and increasing efficiency(see Figure 2.1). Additionally, the lack of physical contact between the vehicle and the guideway means that maglev trains produce significantly less noise than traditional trains, making them a more attractive option for urban areas. This has been demonstrated in the case of the maglev system in Shanghai, China, which operates at a maximum speed of 430 km/h and produces noise levels of only 65 decibels [5].

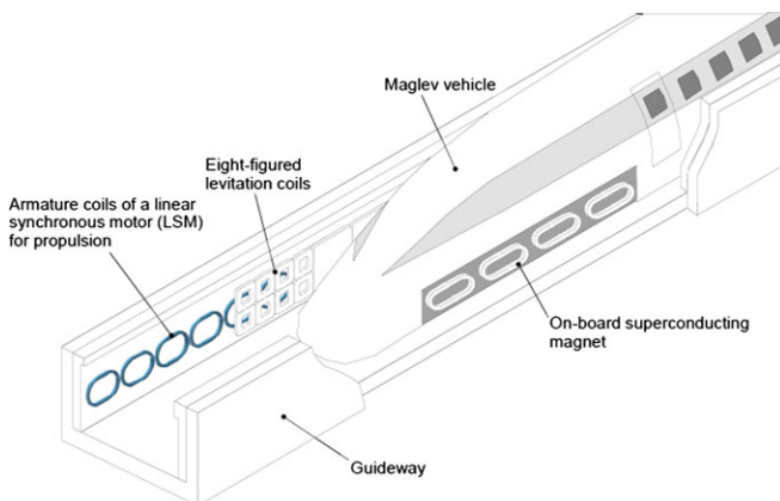


Figure 2.1: Japanese superconducting maglev system L0 expected to be in service in 2027 [4]

Another advantage of maglev technology in transportation is its reduced maintenance costs. Traditional transportation systems such as trains require regular maintenance of tracks, wheels and other components, which can be expensive and time-consuming. Maglev technology, on the other hand, has fewer moving parts and requires less maintenance, resulting in lower costs over the long term [4]. This has been demonstrated in the case of the maglev system in Japan, which has experienced minimal downtime and maintenance costs since its opening in 1997 [5].

Although magnetic levitation has many advantages over conventional transportation systems, it also has some drawbacks. One of the main concerns is the high initial cost of building a maglev system, which can be a barrier to entry for many countries and cities. Additionally, the need for specialized infrastructure and maintenance can also add to the overall cost. Another potential

issue is the limited load capacity of maglev trains, which can be a disadvantage for transporting heavy goods. Finally, the lack of compatibility with existing rail networks and regulations can also pose a challenge for implementing maglev technology on a large scale.

2.2.2 Maglev in microrobotics

The use of magnetic levitation in microrobotics has become a popular research area in recent years, as it provides a non-contact and highly controllable method for manipulating tiny objects. Magnetic levitation has been used in a variety of microrobotic applications, including micromanipulation and biomedical applications.

One of the key advantages of magnetic levitation in microrobotics is the ability to manipulate objects with high precision and without physical contact. This makes it an ideal method for applications such as micromanipulation, where even a small amount of physical contact can cause damage to delicate structures. Khamesee et al. demonstrate this in [6] by using their microrobotic system to pick up and manipulate tiny objects such as metal beads and microspheres.

Another potential application of magnetic levitation in microrobotics is in the field of biomedical engineering. In [7], several examples of microrobotic systems that have been developed for biomedical applications are described. Some of them are drug delivery, cell manipulation and tissue engineering, as is specified in Subsection 2.2.3. Magnetic levitation allows for precise and non-invasive manipulation of biological samples, which can be especially useful for applications where contact with the sample needs to be minimized.

One of the challenges in designing microrobotic systems using magnetic levitation is the need for precise control over the magnetic fields used to levitate and manipulate objects. As research in this field continues, new designs and control strategies will likely be developed to further improve the precision and versatility of microrobotic systems.

2.2.3 Maglev in healthcare

As can be seen in [8], magnetic levitation has many potential applications in the field of medicine. One such application is the separation of biological cells, which can be accomplished using magnetic levitation techniques: by applying a magnetic field to a solution containing cells, the cells can be separated based on their magnetic susceptibility. This technique has been used in various medical applications, such as isolating cancer cells for analysis and diagnosis.

Magnetic levitation can also be used in drug delivery systems. In [8], it is noted that magnetic levitation can be used to guide drug-delivering nanoparticles to specific areas in the body. By using an external magnetic field to control the position of the nanoparticles, they can be directed to the target area, increasing the efficacy of the treatment while minimizing potential side effects.

Furthermore, magnetic levitation has also been explored for the development of tissue engineering techniques. Magnetic levitation can be used to control the position and orientation of cells in a three-dimensional environment, which is critical for the development of functional tissues. By using magnetic levitation to guide the cells, it is possible to create engineered tissues with specific structures and functions. These tissues can be used for a variety of applications, including drug testing, disease modeling, regenerative medicine and even transplantation. They allow researchers to study the effects of drugs and diseases on tissues in a controlled environment, which can lead to the development of more effective treatments. In some cases, engineered tis-

sues may even be suitable for transplantation, although more research is needed in this area [8].

2.2.4 Maglev in magnetic bearings

Magnetic levitation technology has found various applications in the field of bearings. Magnetic bearings offer several advantages over traditional mechanical bearings, including reduced wear and tear, high-speed rotation capabilities and increased energy efficiency. While magnetic bearings were once considered exotic and only used in high-end applications, advancements in magnetic levitation technology have made them more practical and cost-effective. The levitation of rotors using magnetic bearings is achieved by controlling the magnetic fields generated by a set of permanent magnets and electromagnets. This method enables the rotors to rotate without making contact with any physical surfaces, allowing for a stable and efficient operation[5].

Apart from improved efficiency, magnetic bearings also offer reduced maintenance costs, noise reduction and increased durability. They are more resistant to external vibrations and shocks, making them suitable for use in sensitive equipment such as spacecraft and satellites. Despite their benefits, magnetic bearings do come with their set of challenges. Their complexity and high costs can pose difficulties in maintenance and repair and they may require specialized knowledge and equipment for installation and operation.

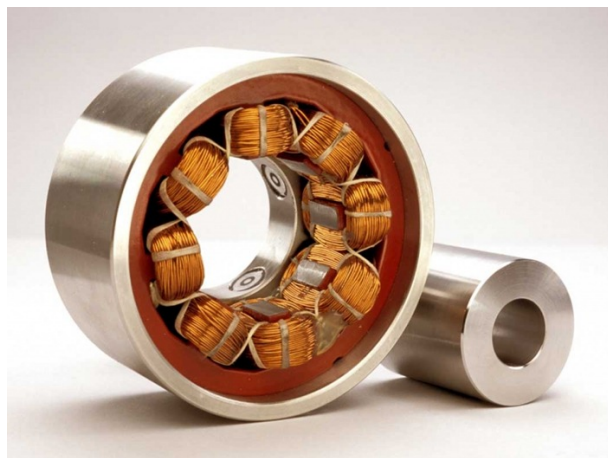


Figure 2.2: Magnetic bearing [9]

2.2.5 Maglev in education

Magnetic levitation technology has proven to be a valuable tool in education, offering a unique and engaging way for students to learn about electromagnetism, control systems and mechanics. Through Maglev experiments, students can explore and demonstrate various theories and concepts related to these fields. With modern Maglev technology becoming more affordable and accessible, there are now opportunities to create low-cost Maglev systems that can be used as educational prototypes. Such systems can be used in classrooms or as a platform for students to gain hands-on experience in designing and controlling Maglev systems.

This project aims to develop a low-cost Maglev prototype system that can be used as an educational tool. The prototype will serve as a model for exploring electromagnetism and testing control loops, making it an excellent tool for teaching students about the fundamentals of mag-

netic levitation technology. The focus will be on designing a system that is simple, affordable and accessible.

2.3 Existing low-cost magnetic levitation systems

As has been seen, magnetic levitation is a very interesting technology due to its wide range of applications. However, magnetic levitation can be expensive due to the need for sophisticated equipment and components. For this reason, low-cost magnetic levitation prototypes have been developed using accessible technology and inexpensive materials.

One of the most important aspects to consider in these prototypes is the type of sensor used to measure the position of the levitating magnet, as this sensor is in charge of providing the necessary information to control the magnetic field and keep the magnet in its levitation position. Furthermore, two other relevant aspects to bear in mind are, on the one hand, the type of levitation i.e. if it works either by attraction or repulsion and, on the other hand, the microcontrollers or computers used to implement and apply the system controller.

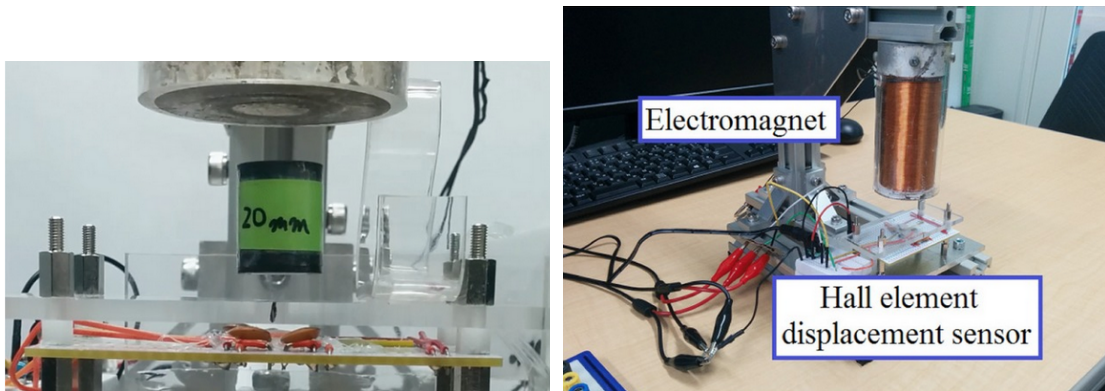


Figure 2.3: Magnetic levitator prototype from [10]

In this section, some of the existing low-cost magnetic levitation prototypes will be briefly presented, highlighting their differences and similarities in terms of technology, materials and structure. In particular, four prototypes that represent the most commonly used possibilities in low-cost prototypes will be described.

The first prototype seen in Figure 2.3 is built using a metal structure and utilizes three Hall-effect sensors as feedback sensors to measure the position of the levitating magnet. The levitating magnet floats between these sensors and the electromagnet and a PC is used to implement the control loop. It is worth noting that a Hall-effect sensor measures the intensity of the magnetic field, so the levitating object in this case is a magnet. The sensor reading is proportional to the distance between the magnet and the sensor. This prototype uses attraction as the levitation force [10].

The second prototype (Fig. 2.4) uses repulsion as the levitation force and requires 12 coils and 3 optical sensors, specifically photodiodes. Photodiodes can detect changes in light intensity and they are used to detect the position and orientation of the levitating object. If the object starts to move away from its desired levitation height, the amount of light hitting the photodiode changes, causing a different electrical response. This change in response can be used to

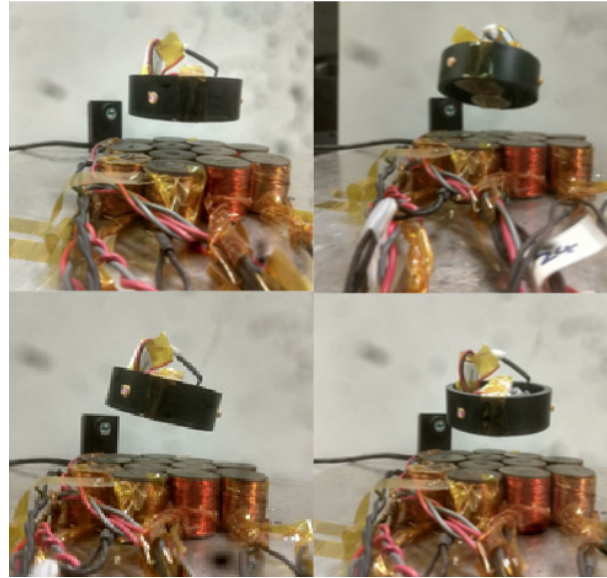


Figure 2.4: Magnetic levitator prototype from [11]

signal the controller that the levitating object has moved from its desired position and requires adjustment, providing feedback to the control system. Moreover, a PC with a Core i5 processor with four cores and Linux operating system is used to implement the control loop [11].

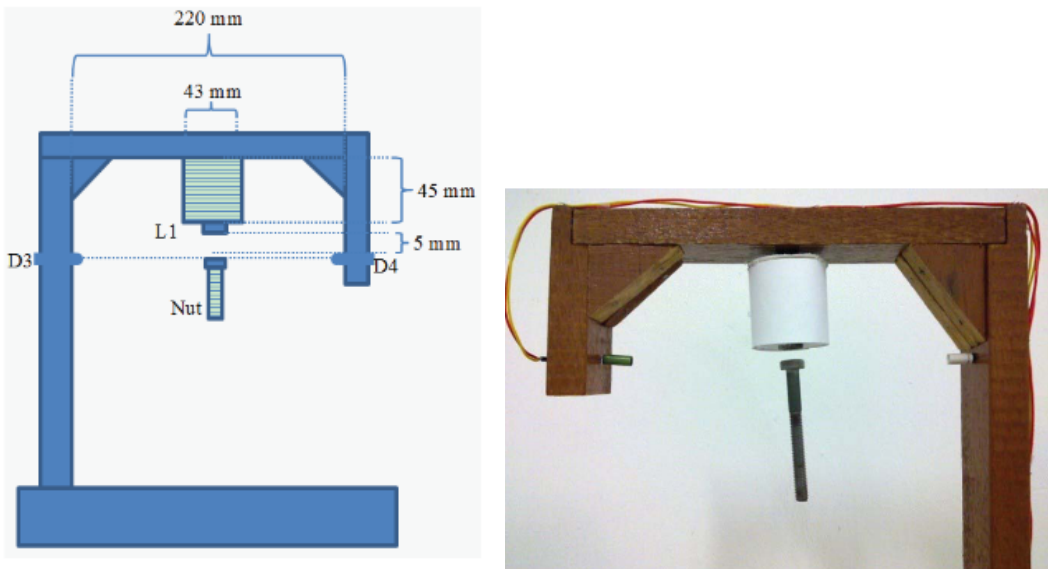


Figure 2.5: Magnetic levitator prototype from [12]

The third prototype is a very simple design (see Fig. 2.5) that uses an infrared sensor to detect the object to be levitated. It uses a PIC microcontroller, which switches current to the electromagnet ON or OFF based on whether the sensor detects the presence of an object or not. This prototype also uses attraction as the levitation force and has a structure similar to the first prototype but it is made of wood [12].

The fourth and final representative prototype (see Figure 2.6) also uses attraction as the levi-

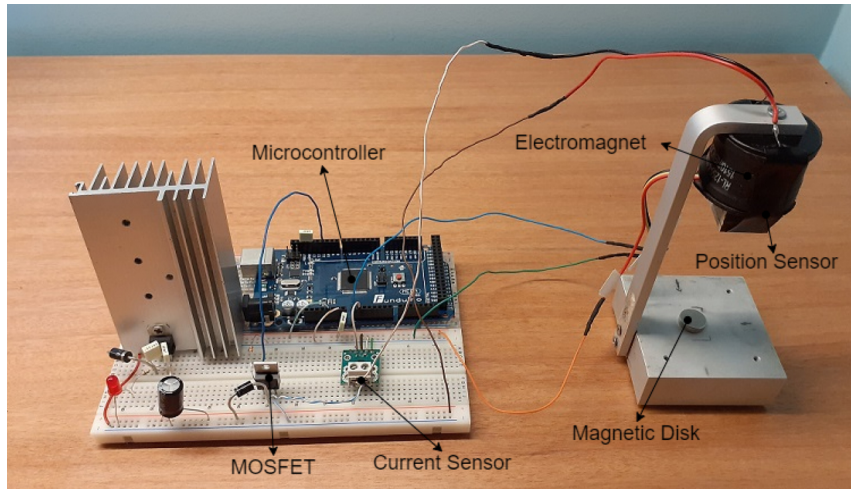


Figure 2.6: Magnetic levitator prototype from [13]

tation force and utilizes a copy of the **Arduino Mega 2560** microcontroller to generate a PWM signal based on the current it wants to send to the coil and the magnetic field it wants to generate in it. It uses a **Hall-effect sensor** to provide feedback of the levitating magnet position and a **MOSFET** to energize the electromagnet, as the Arduino alone would not be able to provide enough current to the coil [13].

This gives an idea of structures, sensors and controllers that can be used to develop this project. The specific decisions made on the design of this project's levitator are made in the following chapter.

Chapter 3

Design and construction of the magnetic levitation prototype

This chapter provides a comprehensive overview of the design process for creating a low-cost and efficient levitator. Each component was carefully considered to ensure cost-effectiveness. Following this criteria, the use of a repulsion-based levitator was quickly discarded due to the higher cost associated with using multiple coils. Consequently, the final decision was to construct an attraction-based structure to minimize costs.

Regarding the sensor selection, a Hall effect sensor was chosen. The decision to use a Hall effect sensor was primarily based on the need to study the system using a magnet as the levitating object. This introduces an additional force with respect to a non-magnetic levitating object as well as complexity to the system. For a non-magnetic object, optical or infrared sensors can be used to measure position. However, considering a magnet as the levitating object introduces the possibility of using a Hall-effect sensor. This sensor measures the intensity of the magnetic field, which is directly proportional to the magnet's position. The Hall effect is more suitable for this application as it is more reliable to sense the position of a magnet. Optical sensors are affected by ambient light and infrared ones are affected by the reflection of light in other surfaces different from the levitating object. Thus, understanding the system's requirements, the final decision was to use a Hall effect sensor.

In choosing a microcontroller for the levitator, an Arduino Uno was selected. This decision was made after considering several factors, including cost, accessibility, and ease of use. One of the reasons was to ensure that the levitator could function independently of a large computer, making it more convenient and portable for laboratory settings or educational environments. The Arduino Uno is affordable, widely available, and comes with an abundance of documentation and open-source code. Moreover, it is a versatile microcontroller that can be used to build a wide range of projects, making it an excellent tool for educational purposes.

The following sections delve into the details of each component to understand their role in the overall system.

3.1 Fabrication of the structure

To build the structure of the prototype, taking into account that the intention was to manufacture a levitator based on attraction, a similar design to the one shown in figure 2.6 was chosen, given its simplicity. Basically, the structure had to fulfil two functions; on the one hand, it had to include a box containing the electronic boards used, that was also close to the sensor and the electromagnet so as not to have to use long cables. On the other hand, a piece that would allow the electromagnet to be supported at a certain height so that the permanent magnet could be suspended underneath.

A 3D design program called Solidworks was used to manufacture the levitator structure. Each of the parts of the prototype has been designed in this program, including the container box and an L-shaped support consisting of a mast and a bridge to hold the electromagnet (see Figure 3.1) at a height of 150mm to allow its action by attraction.

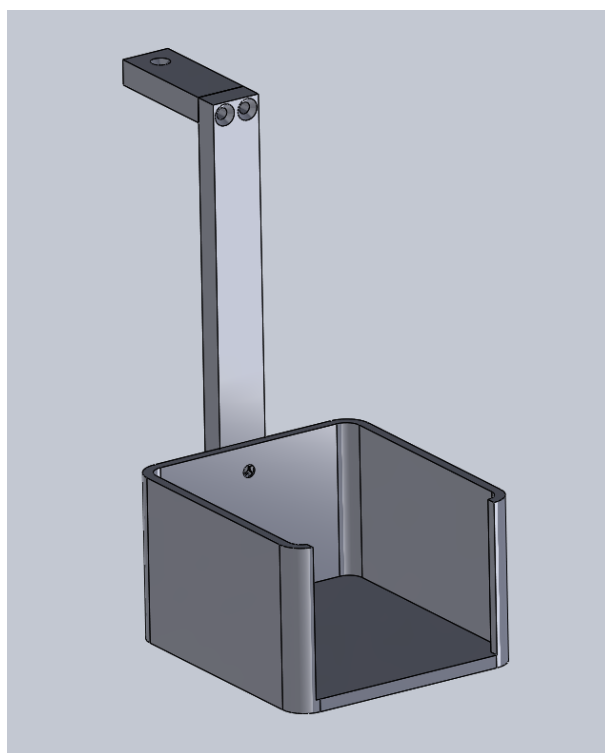


Figure 3.1: Solidworks design of the levitator prototype

The mast and support bridge are made from a calibrated aluminium handrail (a material that does not give problems with respect to the electromagnetic phenomena of the system), which has been machined in a CNC milling machine to make metric 4 drills with countersunk holes to assemble the parts, i.e. to screw the electromagnet to the support bridge and to screw the aluminium L structure to the Arduino container box. This structure allows the boards (Arduino and Motorshield) to be close to the electromagnet and does not require long cables to make the necessary connections.

The box, on the other hand, was made in PLA because of its size and since 3D printing would allow a second modified copy to be printed if necessary. In any case, its size already offers the necessary stability and weight to the prototype, so it was not necessary to make it in aluminium.

The box being printed can be seen in the following Figure:

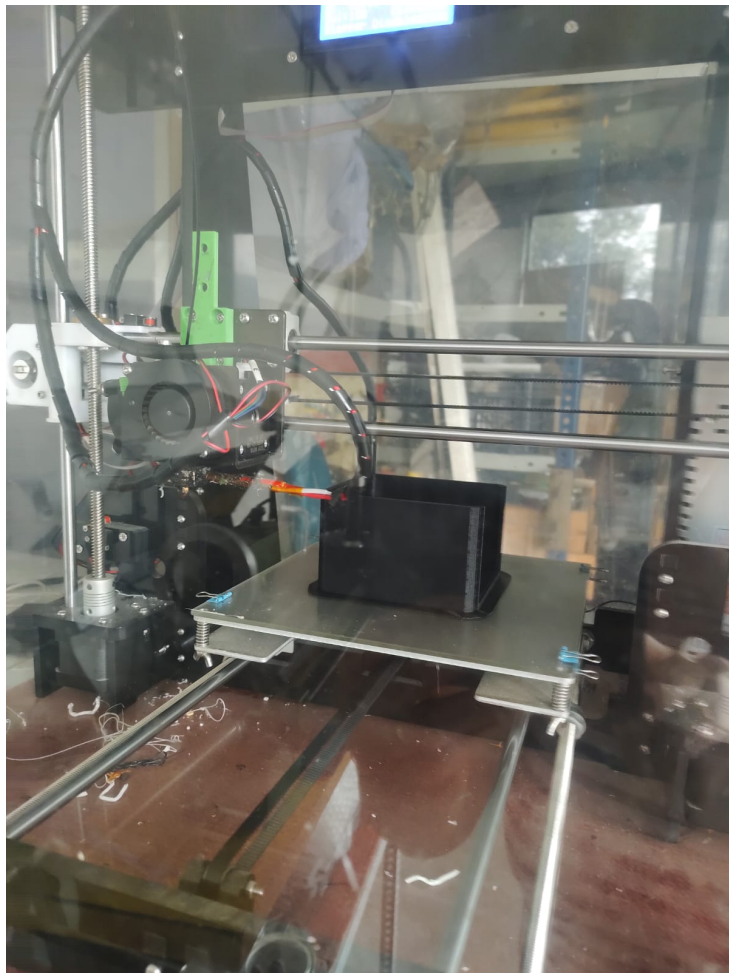


Figure 3.2: Arduino container box being 3D printed

In summary, the levitator structure was manufactured by designing each of the parts in Solid-works, machining the aluminium handrail on a CNC milling machine, 3D printing the PLA container box and assembling the mast, the support bridge and the box containing the boards. The resulting prototype can be seen in Figure 3.3.



Figure 3.3: Constructed structure

3.2 Arduino Uno

The Arduino Uno is an open source electronic prototyping platform based on an ATmega328P microcontroller. It was developed in 2005 by Massimo Banzi's team at the Interaction Design Institute Ivrea (Italy) as an easy-to-use and low-cost tool for programming and controlling electronic devices [14].

The Arduino Uno board is small and features a series of input and output pins that allow the connection of sensors, actuators and other electronic components. These pins can be programmed to perform a variety of tasks, such as reading data from sensors, controlling motors and lights, among other functions [15].

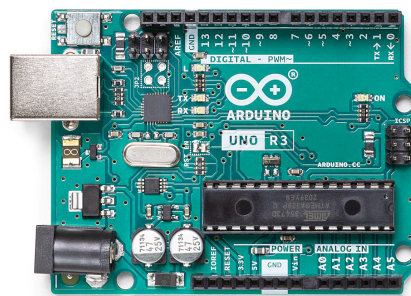


Figure 3.4: Arduino board [15]

The Arduino Uno board includes a USB port that allows communication with a computer to upload programs and receive data. In addition, it has a built-in voltage regulator that allows the board to be powered by an external power supply [15].

One of the main advantages of the Arduino Uno is its ease of use. No prior knowledge of electronics or programming is required to get started. The software used to program the Arduino Uno is free and open source, allowing the creation of a wide variety of electronics and robotics projects.

In conclusion, the Arduino Uno is a versatile, easy-to-use and low-cost electronic prototyping platform that allows the programming and control of electronic devices in a simple way.

For the particular case of the prototype of this project, the Arduino has been connected to a 12V power supply through the jack connector as this is the voltage required by the electromagnet to operate and has also been used to program the different algorithms to control the system in a closed loop.

3.3 Hall-effect sensor

For this prototype a 49E Hall effect sensor has been chosen. It is a low-cost, widely available device commonly used for detecting magnetic fields. It operates on the principle of the Hall effect, which produces a voltage proportional to the strength and direction of the applied magnetic field. The sensor is small and lightweight, making it suitable for use in compact systems like this prototype [16].



Figure 3.5: Hall effect sensor pinout [16]

The 49E Hall Effect sensor is used in the magnetic levitation system to measure the position of the levitating magnet. To do so, it has been positioned just below the center of the electromagnet at a distance of 5mm. The sensor provides an analog voltage signal that is proportional to the strength of the magnetic field generated by the magnet. This information is used by the feedback control algorithm to adjust the current supplied to the electromagnet, maintaining the levitation of the magnet at a fixed position.

Overall, the 49E Hall effect sensor is a practical and cost-effective solution for magnetic field sensing applications such as this one.

3.4 Levitator electromagnet

The electromagnet is the central component of the magnetic levitation prototype, responsible for generating the magnetic field that attracts the magnet and enables levitation. It consists of a coil of wire wound around a ferromagnetic core.

The strength of the magnetic field generated by the electromagnet is determined by the current flowing through the coil. To achieve precise control of the magnetic field strength, the current is regulated by the motor shield board, which is connected to the electromagnet. The selection of a 12V electromagnet was based on the voltage rating of the coil, which is screwed into the supporting bridge of the aluminum L of the prototype. It is exactly as the one seen in the following figure except for its voltage specification:



Figure 3.6: Heschen electromagnet [17]

When a direct current flows through the coil, it creates a magnetic field that is strong enough to overcome the force of gravity acting on the magnet and causes it to levitate. Therefore, the successful operation of the electromagnet depends on the precise regulation of the current flowing through the coil, which is achieved through the motor shield board.

In summary, the electromagnet's operation is critical to the magnetic levitation prototype and its magnetic field strength is precisely controlled through the motor shield board, which regulates the current flowing through the coil.

3.5 Arduino motorshield

To make an electromagnet work, a current magnitude higher than what the simple Arduino board can provide is necessary, which would be a few mA. The same would be true for a DC motor. In fact, the Arduino company itself has developed a specific board (or shield) to address this problem precisely to drive small DC motors. It is called Arduino Motorshield Rev3 and can be used as the power stage for the electromagnet.

The Arduino Motor Shield Rev3 is designed to work with an Arduino board and provide a simple way to control DC motors and other inductive loads like electromagnets. The shield has two motor drivers that are capable of driving two DC motors or one stepper motor. Each driver consists of two MOSFETs that can switch the polarity of the motor's power supply to control the

direction of the motor's rotation. The shield also includes two current sense resistors to measure the current flowing through each motor [18].

To use the shield, the electromagnet must be connected to the shield's screw terminals, connect the control pins to the Arduino board's pins and power the shield using either an external power supply or the Arduino board's Vin pin. In this case, the board has been powered through the Arduino Uno jack which feeds both circuits at 12V, as with this voltage it can provide up to 2 amps of current to the coil.

Once the shield is powered on, the motor control pins must be set. The Arduino Motor Shield Rev3 uses 8 of the Arduino board's pins to drive or sense motors, divided into two channels labeled A and B. Each channel uses 4 pins for its various functions. Channel A and Channel B can be used independently to control two DC motors. The pins associated with each channel are as follows: for Channel A, the Direction pin is D12, the PWM pin is D3, the Brake pin is D9, and the Current Sensing pin is A0; for Channel B, the Direction pin is D13, the PWM pin is D11, the Brake pin is D8, and the Current Sensing pin is A1 [18].

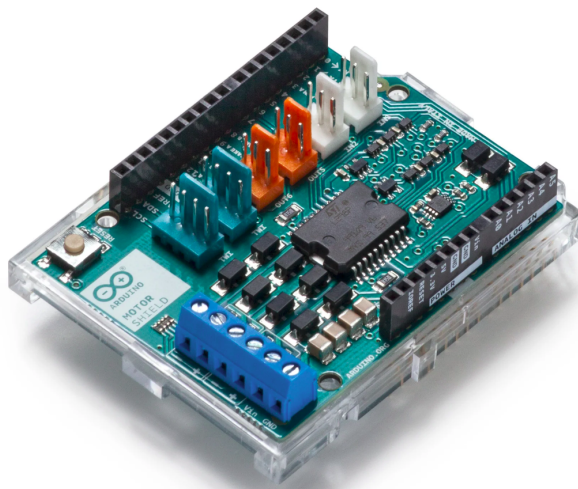


Figure 3.7: Arduino motorshield Rev3 [18]

In order to control the electromagnet, then, channel A has been chosen. So, digital pin 12 has been used to control the polarity of the voltage applied to the electromagnet. This will determine the direction of the magnetic field generated by the coil. And through digital pin 3 the duty cycle of the PWM signal to control the current flowing through the electromagnet is set. The other pins have not been used.

The Pulse Width Modulation (PWM) signal is a widely used technique for controlling the amount of power delivered to a load by varying the width of a pulse of electrical energy. In PWM, a series of pulses is generated, with the duration of each pulse controlled by a digital signal, such as from an Arduino or other micro-controller. By varying the width of the pulses, the average voltage or current delivered to the load can be adjusted, which in turn can control the speed of a motor or the current through a coil. The basic idea behind PWM is to turn the power on and off rapidly, creating a waveform that has a varying duty cycle (the percentage of time the power is on during each cycle). For example, if the waveform has a 50% duty cycle, the power will be on for half of the cycle and off for the other half. By adjusting the duty cycle, the

average power delivered to the load can be varied, allowing for precise control over its operation [19].

Overall, the Motorshield Rev3 provides a convenient and reliable way to power and control the electromagnet in the levitation prototype.

3.6 Complete system

So, overall, the magnetic levitation prototype was designed and constructed with the aim of achieving stable levitation of a magnet using an attractive magnetic levitation system. The system is controlled by an Arduino Uno microcontroller board, which executes a feedback control algorithm based on the output from a 49e Hall effect sensor. The prototype consists of a 3D printed box that houses the Arduino Uno board and provides a protective enclosure for the electronics. The electromagnet is mounted on an aluminum L-shaped bracket that is attached to the side of the containment box. The magnet, which is the levitating object, is placed below the electromagnet and is free to move in the vertical direction.

As the levitation is based on attraction, the Hall effect sensor is positioned directly underneath the center of the electromagnet, at a distance of 5mm, in order to detect the magnetic field generated by the magnet. The sensor outputs an analog voltage signal that is proportional to the strength of the magnetic field.

The control algorithm implemented on the Arduino Uno board reads the sensor output and adjusts the current supplied to the electromagnet to maintain the levitation of the magnet at a fixed position. With the aluminum bracket securely attached to the containment box, the prototype is capable of sustaining stable levitation of the magnet. The whole prototype assembled and working can be seen in Figure 3.8.

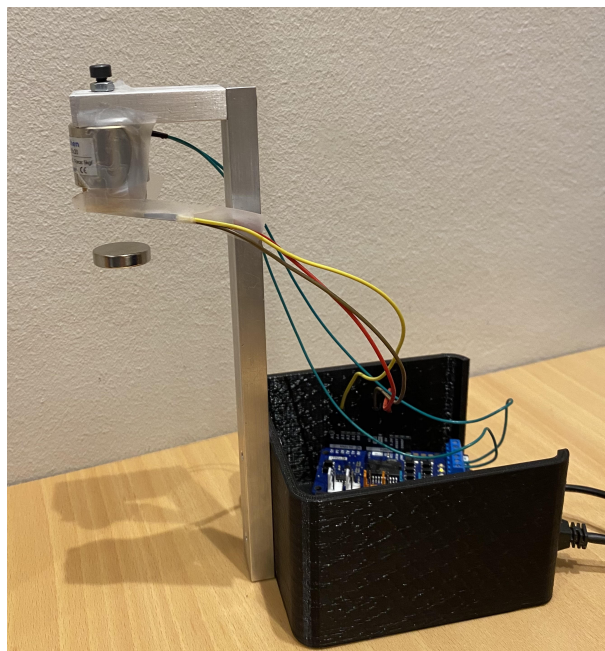


Figure 3.8: Assembled and working levitator

Chapter 4

Dynamic modeling of the Magnetic Levitation System

To develop an effective control strategy that can ensure the stability of the system, a detailed analysis of the dynamics of a magnetic levitation system is provided in this chapter. First of all, the physical principles underlying the system are studied in order to derive a model that approximates the system dynamics.

Once the dynamic equations that explain the system behavior have been extracted, the state space representation of the system will be obtained. Subsequently, the system will be linearized around an equilibrium point, as this will be necessary for the design of the control algorithm.

4.1 Dynamic equations of the system

It is necessary to know the dynamic model of the system in order to be able to proceed to design a control system. For this reason, this section will be devoted to obtaining the model by studying the physical phenomena that are the basis of this system. The dynamic behavior of the magnetic levitation system can be described by a set of nonlinear differential equations that govern the motion of the levitating magnet. The derivation of these equations will be outlined using the principles of electromagnetism and Newtonian mechanics.

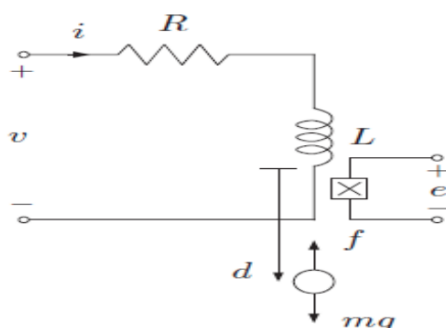


Figure 4.1: Model of the magnetic levitation system [20]

According to the system diagram shown in Figure 4.1, the dynamics of the system can be separated into two parts: the electrical part, which deals with the physics of the electromagnet and the mechanical part, which deals with the balance of forces between the gravity and the magnetic forces experienced by the levitating magnet.

4.1.1 Mechanical part

With regard to the mechanical part, it is worth remembering the following Newton's law $\sum F = m \cdot a$, which states that the sum of forces acting on an object is directly proportional to its mass and acceleration. In other words, if a force F is applied to an object with mass m , the object will accelerate in the direction of the force with an acceleration $a = F/m$.

If this law is applied to the magnet that is to be levitated, two forces affect it: **the force of gravity** ($m \cdot g$) and **the magnetic force due to the electromagnet**. The latter is defined by the following equation[20]:

$$k_v \cdot \frac{i^2}{z^2}$$

Where k_v is a constant related to the magnetic force, i is the current through the coil and z is the position of the magnet relative to the lowest part of the coil. So going back to Newton's law, it is obtained (considering the positive sense of z downwards):

$$m \cdot g - k_v \cdot \frac{i^2}{z^2} = m \cdot \dot{v} \quad (4.1)$$

Being v the speed of the magnet.

This equation relates the acceleration of the levitating object to a few different forces: the force of gravity and the force generated by the magnetic field acting on the object. This second term shows how, as the object gets closer to the magnetic field, the force becomes stronger and as it moves further away, the force becomes weaker. The negative sign in front of the $k_v \cdot \frac{i^2}{z^2}$ term means that the force is directed towards the magnetic field, opposing the force of gravity. So, this force causes the object to accelerate upwards.

4.1.2 Electrical part

Regarding the electrical dynamics of the system, it is necessary to take into account both **Ohm's law** and **Faraday's law of electromagnetic induction**. The circuit consists of a power source that drives a coil of wire (the electromagnet), which generates a magnetic field that interacts with a magnet (the levitating magnet) that is placed above it. The **coil of wire includes a resistor (R) and an inductor (L)** and is driven by a voltage source (u). The current flowing through the coil is denoted by i . So, to describe **how the current changes over time** in this system, three terms need to be considered:

- The first term represents the effect of the **resistance** in the circuit, which tends to reduce the current over time: $-\frac{R}{L} \cdot i$
- The second term represents the effect of the **input voltage** u , which tends to increase the current: $\frac{1}{L} \cdot u$
- And finally, the third term represents the effect of the **motion of the levitating magnet below** an electromagnet. This term is derived from **Faraday's law** which states that a

changing magnetic field can induce voltage in a conductor. In this case, the motion of the levitating magnet induces a voltage in the coil of the electromagnet, which opposes the flow of current in the coil and reduces it.

The magnitude and direction of the induced voltage depends on the velocity(v) and position(z) of the levitating magnet, as well as the geometry and material properties of the system: $-\frac{k_m}{L} \cdot \frac{z \cdot v}{(r^2 + z^2)^{\frac{5}{2}}}$. The negative sign in the term indicates that the induced voltage opposes the flow of current in the coil, in accordance with Faraday's law.

The coefficient $\frac{k_m}{L}$ represents the coupling between the magnetic and electrical dynamics of the system. In particular, k_m is calculated using a formula that involves the mass m of the levitating magnet, the number of turns of the coil N and the radius of the coil r , as well as the vacuum permeability (μ_0): $k_m = \frac{3}{2} \cdot \mu_0 \cdot m \cdot N \cdot r^2$.

In short, the equation describing the change in current with respect to time, considering all terms, is as follows:

$$\dot{i} = \frac{-R}{L} \cdot i + \frac{1}{L} \cdot u - \frac{k_m}{L} \cdot \frac{z \cdot v}{(r^2 + z^2)^{\frac{5}{2}}} \quad (4.2)$$

4.2 State space representation of the system

To represent the system as a state space model, the state variables, the input to the system and the output to be measured must be considered:

$$\begin{bmatrix} x_1 \\ x_2 \\ x_3 \end{bmatrix} = \begin{bmatrix} z \\ v \\ i \end{bmatrix}; \quad u = u; \quad y = z$$

If the derivatives of these state variables are isolated, the equations of the system are as follows:

$$\dot{z} = v \quad (4.3)$$

$$\dot{v} = g - \frac{k_v}{m} \cdot \frac{i^2}{z^2} \quad (4.4)$$

$$\dot{i} = -\frac{R}{L} \cdot i + \frac{1}{L} \cdot u - \frac{k_m}{L} \cdot \frac{z \cdot v}{(r^2 + z^2)^{\frac{5}{2}}} \quad (4.5)$$

That is, in matrix form, it follows that:

$$\begin{bmatrix} \dot{x}_1 \\ \dot{x}_2 \\ \dot{x}_3 \end{bmatrix} = \begin{bmatrix} x_2 \\ g - \frac{k_v}{m} \cdot \frac{x_2^2}{x_1} \\ -\frac{R}{L} \cdot i + \frac{1}{L} \cdot u - \frac{k_m}{L} \cdot \frac{x_1 \cdot x_2}{(r^2 + x_1^2)^{\frac{5}{2}}} \end{bmatrix} \quad (4.6)$$

Since the system being described is non-linear, it cannot be represented by a constant A state matrix. One possible strategy to obtain a state space representation is to use the Taylor series linearisation method. This method allows the behaviour of the non-linear system to be approximated around an operating point by expanding its equations in power series and retaining terms up to first order.

4.3 Linearization of the system

The Taylor series linearisation method is a technique commonly used to approximate the behaviour of non-linear systems at a specific operating point. The objective is to obtain a linear representation of the system, which is easier to analyse and control.

The idea is to approximate the non-linear functions of the system by their power series expansions around the operating point and then truncate the series to a sufficiently high order to obtain a good approximation. The result is a linearised model of the system, which can be represented in state space and analysed using standard control techniques.

To apply this method to the system being described, it is first necessary to identify an operating point around which the linearisation will be performed. To find the point of equilibrium, the equations of the system must be solved when $\dot{z} = \dot{v} = \dot{i} = 0$. For now, the equilibrium point is set to $v = 0$ since what is expected is to keep the magnet levitating at one point in a stable way. Since there are some parameters of the system that are not yet known, it is not possible to simply calculate u , z and i at equilibrium by equating their derivative to zero. Therefore, they have been found empirically by implementing the PID in chapter 5. So, at this point, it is possible to refer to u^* , z^* and i^* and their value will be specified later.

Once the operating point has been identified, the Taylor series expansions of the non-linear functions of the system around that equilibrium point must be obtained. Being $f_1(z, v, i, u)$, $f_2(z, v, i, u)$ and $f_3(z, v, i, u)$ the non-linear functions corresponding to the first, second and third equations of the system respectively, the Taylor series expansions (ignoring the non-linear terms) can be written as:

$$\begin{aligned}\dot{z} &= f_1(x, u) \approx f_1(x^*, u^*) + \frac{\partial f_1}{\partial z} \Big|_{x^*, u^*} (z - z^*) + \frac{\partial f_1}{\partial v} \Big|_{x^*, u^*} (v - v^*) + \frac{\partial f_1}{\partial i} \Big|_{x^*, u^*} (i - i^*) + \frac{\partial f_1}{\partial u} \Big|_{x^*, u^*} (u - u^*) \\ \dot{v} &= f_2(x, u) \approx f_2(x^*, u^*) + \frac{\partial f_2}{\partial z} \Big|_{x^*, u^*} (z - z^*) + \frac{\partial f_2}{\partial v} \Big|_{x^*, u^*} (v - v^*) + \frac{\partial f_2}{\partial i} \Big|_{x^*, u^*} (i - i^*) + \frac{\partial f_2}{\partial u} \Big|_{x^*, u^*} (u - u^*) \\ \dot{i} &= f_3(x, u) \approx f_3(x^*, u^*) + \frac{\partial f_3}{\partial z} \Big|_{x^*, u^*} (z - z^*) + \frac{\partial f_3}{\partial v} \Big|_{x^*, u^*} (v - v^*) + \frac{\partial f_3}{\partial i} \Big|_{x^*, u^*} (i - i^*) + \frac{\partial f_3}{\partial u} \Big|_{x^*, u^*} (u - u^*)\end{aligned}$$

To obtain the state space equations, each of these terms must be calculated. From this point on, x and u will be referred to as: $x = x - x^*$ and $u = u - u^*$. Since, as mentioned above, at the equilibrium point $\dot{x} = 0$, $f_1(x^*, u^*)$, $f_2(x^*, u^*)$ and $f_3(x^*, u^*)$ terms are zero. Being $f_1(x, u) = v$, $f_2(x, u) = g - \frac{k_v}{m} \cdot \frac{i^2}{z^2}$ and $f_3(x, u) = -\frac{R}{L} \cdot i + \frac{1}{L} \cdot u - \frac{k_m}{L} \cdot \frac{z \cdot v}{(r^2 + z^2)^{\frac{5}{2}}}$, the remaining terms are developed below:

$$\frac{\partial f_1}{\partial z} \Big|_{x^*, u^*} = \frac{\partial f_1}{\partial i} \Big|_{x^*, u^*} = \frac{\partial f_1}{\partial u} \Big|_{x^*, u^*} = 0; \quad \frac{\partial f_1}{\partial v} \Big|_{x^*, u^*} = 1$$

$$\frac{\partial f_2}{\partial v} \Big|_{x^*, u^*} = \frac{\partial f_2}{\partial u} \Big|_{x^*, u^*} = 0; \quad \frac{\partial f_2}{\partial z} \Big|_{x^*, u^*} = 2 \cdot \frac{k_v}{m} \cdot \frac{i^2}{z^3}; \quad \frac{\partial f_2}{\partial i} \Big|_{x^*, u^*} = -2 \cdot \frac{k_v}{m} \cdot \frac{i}{z^2}$$

$$\frac{\partial f_3}{\partial z} \Big|_{x^*, u^*} = -\frac{k_m}{L} \cdot v \cdot \frac{(r^2 + z^2)^{\frac{5}{2}} - 5 \cdot z^2 \cdot (r^2 + z^2)^{\frac{3}{2}}}{(r^2 + z^2)^5}; \quad \frac{\partial f_3}{\partial v} \Big|_{x^*, u^*} = -\frac{k_m}{L} \cdot \frac{z}{(r^2 + z^2)^{\frac{5}{2}}}$$

$$\frac{\partial f_3}{\partial i} \Big|_{x^*, u^*} = -\frac{R}{L}; \quad \frac{\partial f_3}{\partial u} \Big|_{x^*, u^*} = \frac{1}{L}$$

Therefore, bearing in mind that $v^* = 0$ (i.e. the term $\frac{\partial f_3}{\partial z}$ is cancelled), the state space matrices are:

$$A = \begin{bmatrix} 0 & 1 & 0 \\ 2 \cdot \frac{k_v}{m} \cdot \frac{(x_3^*)^2}{(x_1^*)^3} & 0 & -2 \cdot \frac{k_v}{m} \cdot \frac{x_3^*}{(x_1^*)^2} \\ 0 & -\frac{k_m}{L} \cdot \frac{x_1^*}{(r^2 + (x_1^*)^2)^{\frac{5}{2}}} & -\frac{R}{L} \end{bmatrix}, \quad B = \begin{bmatrix} 0 \\ 0 \\ \frac{1}{L} \end{bmatrix}, \quad C = \begin{bmatrix} 1 & 0 & 0 \end{bmatrix}, \quad D = \begin{bmatrix} 0 \end{bmatrix}$$

4.4 Parameter Estimation

The objective of this section is to estimate the system parameters that appear in the dynamic equations of motion and to find an equilibrium point. This information will allow for the calculation of the numerical A and B matrices necessary to obtain the transfer function of the system, which can be used to analyze and predict the behavior of the system. This is important for accurate modeling and control of the system.

Several parameters of the model could be directly measured, such as the mass of the neodymium magnet, m , which was determined using a scale. The inductance, L and resistance of the coil, R were measured using an LCR meter. Additionally, the radius r and length l of the electromagnet were measured using a caliper. These measured parameters were used to calculate the remaining parameters needed to obtain the transfer function of the system. For instance, to calculate the value of k_m , the number of turns N must first be obtained using the formula $N = \sqrt{L \cdot l / (A \cdot \mu_0)}$, where $A = \pi r^2$ is the circular area of the coil facing the levitating magnet. The value of k_m can then be calculated using the formula $k_m = \frac{3}{2} \cdot \mu_0 \cdot m \cdot N \cdot r^2$ [21]. The values of all parameters are summarized in Table 4.1.

In addition to the measured parameters, there are also known constants required for the system analysis, such as the gravitational acceleration, g , with a standard value of 9.81 m/s^2 and the permeability of free space, μ_0 , with a value of $4\pi \times 10^{-7} \text{ H/m}$.

The equilibrium values x_1^* , x_2^* , x_3^* and u^* were determined empirically through PID control of the prototype. The method used to find a point where levitation was stable is detailed in Chapter

5. From that point the variables at equilibrium were measured. Finally, from this equilibrium point, the last remaining parameter, k_v , could be calculated (see Listing 8.1).

Parameter	Value	Units
m - Mass of the neodymium magnet	0.01	kg
L - Coil inductance	0.056	H
R - Coil resistance	38	Ω
r - Coil radius	0.0125	m
l - Coil length	0.02	m
A - Coil surface facing the magnet	$4.9087 \cdot 10^{-4}$	m^2
N - Number of turns of the coil	1348	-
k_m	$3.9686 \cdot 10^{-9}$	$A \cdot H \cdot m^3$
μ_0 - Permeability of free space	$4\pi \cdot 10^{-7}$	H/m
g - Gravity acceleration	9.81	m/s^2
z^*	0.023	m
v^*	0	m/s
i^*	0.132	A
u^*	7.1	V
k_v	0.003	$N \cdot m^2/A^2$

Table 4.1: System parameters

4.5 Transfer function analysis

Having obtained the system parameters, the state-space matrices of the linearised system are as follows:

$$A = \begin{bmatrix} 0 & 1 & 0 \\ 853.0435 & 0 & -148.6364 \\ 0 & -0.1326 & -678.5714 \end{bmatrix}, \quad B = \begin{bmatrix} 0 \\ 0 \\ 17.8571 \end{bmatrix}, \quad C = \begin{bmatrix} 1 & 0 & 0 \end{bmatrix}, \quad D = \begin{bmatrix} 0 \end{bmatrix}$$

As told, the last part of this section is devoted to [obtain the system transfer function](#) as it provides a convenient way to analyze the system's behavior, stability and performance. This section explains how to derive the transfer function from a state-space representation.

Consider a linear time-invariant (LTI) system represented by the state-space equations:

$$\begin{aligned} \dot{x}(t) &= Ax(t) + Bu(t) \\ y(t) &= Cx(t) + Du(t) \end{aligned}$$

where $x(t) \in \mathbb{R}^n$ is the state vector, $u(t) \in \mathbb{R}^m$ is the input vector, $y(t) \in \mathbb{R}^p$ is the output vector, $A \in \mathbb{R}^{n \times n}$, $B \in \mathbb{R}^{n \times m}$, $C \in \mathbb{R}^{p \times n}$ and $D \in \mathbb{R}^{p \times m}$ are constant matrices.

Then, the Laplace transform is applied to both sides of the state equations, which yields:

$$\begin{aligned} sX(s) &= AX(s) + BU(s) \\ Y(s) &= CX(s) + DU(s) \end{aligned}$$

where $X(s)$, $U(s)$ and $Y(s)$ are the Laplace transforms of $x(t)$, $u(t)$ and $y(t)$, respectively. Substituting $X(s)$ from the first equation into the second equation gives:

$$Y(s) = C(sI - A)^{-1}BU(sU(s) + U(s))$$

And rearranging the terms gives:

$$G(s) = \frac{Y(s)}{U(s)} = C(sI - A)^{-1}B + D$$

where I is the identity matrix and $G(s)$ is the transfer function of the system. The transfer function relates the Laplace transform of the system's output $Y(s)$ to the Laplace transform of its input $U(s)$.

Thus, the transfer function of the magnetic levitation system studied in this project is:

$$G(s) = C(s \cdot I - A)^{-1}B + D = \frac{-2654}{s^3 + 678.6s^2 - 872.8s - 5.789 \cdot 10^5}$$

When implementing a control system on a microcontroller such as the Arduino, it is important to note that the transfer function must be in its discrete form. This is because microcontrollers operate with a finite sampling rate, which means that input and output values are measured and updated at finite, regular time intervals. Therefore, it is necessary to discretise the transfer function before implementing it on the Arduino. This can be done using the bilinear transform.

The basic idea of this transform is to map the poles and zeros of the s (continuous) plane to the z (discrete) plane through a bilinear transformation. This transformation involves replacing s in the continuous transfer function by an expression that involves z [22].

The formula for the bilinear transformation is:

$$s = \frac{2}{T} \cdot \frac{1 - z^{-1}}{1 + z^{-1}}$$

Where T is the sampling time used for the conversion. Once this substitution is made, the continuous transfer function becomes a discrete transfer function, which can be implemented in digital systems.

The sampling time has been approximated by looking at how long it took the Arduino to complete a control loop. So, the sampling time has been set to 2.5ms and the following discrete transfer function was obtained:

$$G(z) = \frac{-4.751 \times 10^{-6}z^2 - 1.317 \times 10^{-5}z - 2.055 \times 10^{-6}}{z^3 - 2.189z^2 + 1.368z - 0.1833}$$

Taking this transfer function and equalling its denominator to 0, we obtain the poles of the discrete system, which are as follows:

poles =

1.0758

0.9296

0.1833

As not all the poles are inside the circle of radius one centred at the origin, it is proved that the levitation system is unstable.

Chapter 5

System control through a PID

This chapter of the project is focused on system control through a PID (Proportional-Integral-Derivative) algorithm. PID control is a widely used method in engineering applications to stabilize system output by controlling system input.

In the context of this magnetic levitation prototype, PID control is used to adjust the current flowing through the electromagnet to maintain a stable levitation height of the magnet. The PID algorithm works by continuously monitoring the height of the magnet and comparing it to a set point.

Based on this comparison, the algorithm calculates an error value, which is then used to adjust the current flowing through the electromagnet. The proportional, integral and derivative gains of the PID controller are set to specific values that optimize the control response and stability of the system.

In this chapter, the implementation of the PID algorithm in the magnetic levitation prototype will be discussed, including the selection of PID parameters and the use of an Arduino microcontroller to execute the control algorithm.

5.1 PID control theory

Proportional-Integral-Derivative (PID) control is a widely used technique in control theory. It involves three components - Proportional (P), Integral (I) and Derivative (D) - each of which contributes to the overall control output in a unique way [22]:

- **Proportional (P):** The proportional component of the PID controller is the most basic and straightforward part of the controller. It simply calculates an output proportional to the error between the desired setpoint and the current process variable. The output of the P component is directly proportional to the size of the error, meaning that as the error increases, so does the output of the P component. The P component is most effective at quickly bringing the process variable to the setpoint, but may result in overshoot and oscillations if the gain is set too high.
- **Integral (I):** The integral component of the PID controller is responsible for reducing the

steady-state error that may exist in the system. It calculates an output proportional to the integral of the error over time and adds it to the output of the P component. The I component is useful in situations where there may be a bias in the system, such as friction or offset, that causes the process variable to settle at a value that is different from the setpoint. The I component will gradually increase the output until the steady-state error is eliminated. However, too much I gain can cause the controller to become unstable and result in overshoot.

- **Derivative (D):** The derivative component of the PID controller is responsible for dampening the response of the controller to sudden changes in the error. It calculates an output proportional to the rate of change of the error and subtracts it from the output of the P and I components. The D component can be useful in situations where there is a need to reduce overshoot or oscillations caused by the P component. However, the D component is sensitive to noise and can amplify noise in the system if the gain is set too high.

In summary, the P component is responsible for responding quickly to changes in the error, the I component reduces steady-state error and the D component dampens the response to sudden changes in the error. A well-tuned PID controller balances the strengths of each component to provide stable and accurate control of the system.

The main advantage of PID control is its simplicity and ease of implementation. It requires minimal computational resources and can be implemented using basic hardware components. Additionally, the flexibility of the PID control algorithm makes it suitable for a wide range of control problems.

However, there are also some disadvantages associated with PID control. The main challenge is tuning the controller parameters (P, I and D) to achieve optimal performance. This process can be time-consuming and requires a good understanding of the system dynamics. Additionally, PID control may not be suitable for systems with highly nonlinear or time-varying dynamics, as it assumes a linear relationship between the control input and the system output.

5.2 PID simulation

This section of the project involves designing a PID controller for a magnetic levitation system. Once the discrete transfer function is obtained, the root locus method is used to design the controller. The transfer function for a PID controller in discrete time is [22]:

$$G(z) = K_p + \frac{K_i}{z} + K_d \frac{(z - 1)}{z}$$

Where K_p , K_i and K_d are the proportional, integral and derivative gains respectively.

To design a PID controller for a discrete-time system using the root locus method, the first step is to obtain the open-loop transfer function of the system in the z-domain. This function describes how the system responds to a change in the input, without any feedback, in discrete time.

Next, the root locus plot of the system in the z-domain must be analyzed. The root locus is a graphical representation of the locations of the closed-loop poles as the gain of the controller varies in the z-domain. The poles are the points where the denominator of the closed-loop

transfer function is equal to zero in the z-domain. In the Matlab graphical representation, these are represented as crosses.

Therefore, the root locus can be used to determine the optimal values of the controller gains that will provide the desired closed-loop response, such as stability, settling time and overshoot, in the z-domain.

Initially, only the proportional gain has been considered as it is the simplest form of control. Figures 5.1 and 5.2 have been obtained using $K_p = -1$. As it can be seen, there is a pole outside the unit circle and no gain value could make it stable. Therefore, it can be concluded that indeed a P-controller is not sufficient to control this magnetic levitation system.

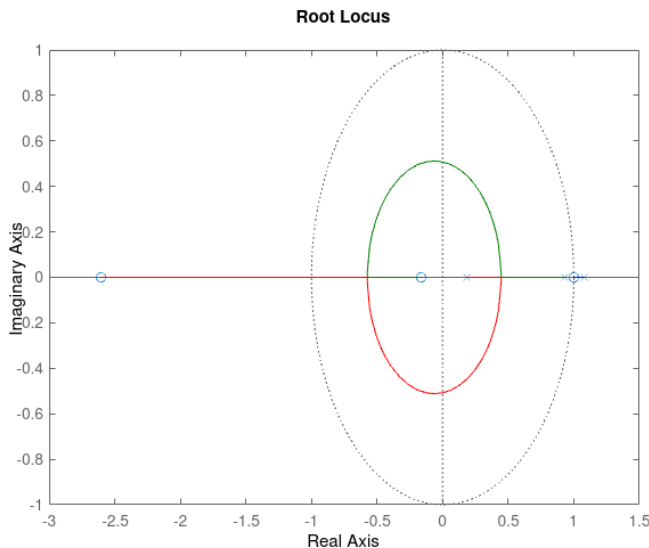


Figure 5.1: Root locus of the system with P controller

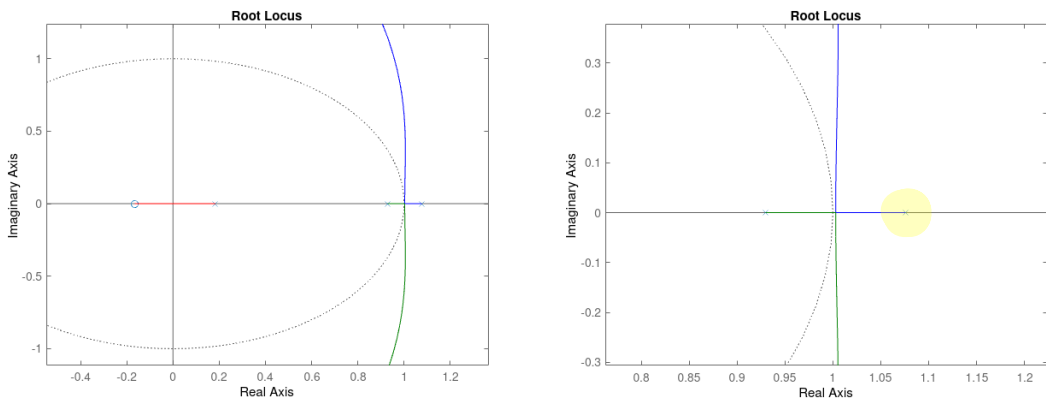


Figure 5.2: Detail of the root locus with P controller

Therefore, to further improve the system response in the z-domain K_i or K_d can be added. The result of adding only K_i is the same as for the P controller, so the simpler controller found that stabilizes the system is a PD. Looking at the figures 5.3 and 5.4, it can be seen that for a gain of

226 the **unstable pole would become stable**. In particular, for that gain, the system would have a 0% overshoot and real poles, so the response is not expected to oscillate when reaching steady state.

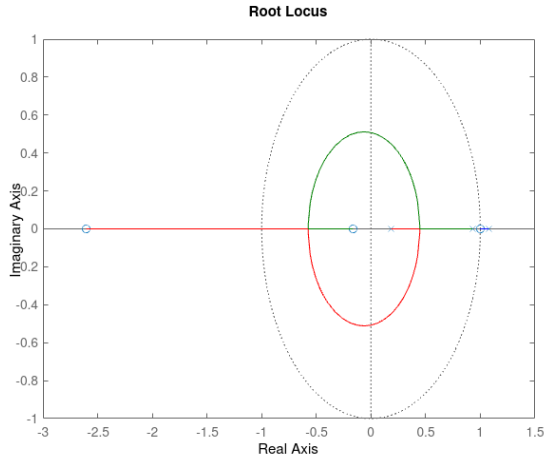


Figure 5.3: Root locus of the system with K_p and K_d

In particular, using Matlab, it has been found that the closed-loop poles with $K_p = -220$ and $K_d = -1$ are:

```
poles =
0.9970
0.9844
0.1875
```

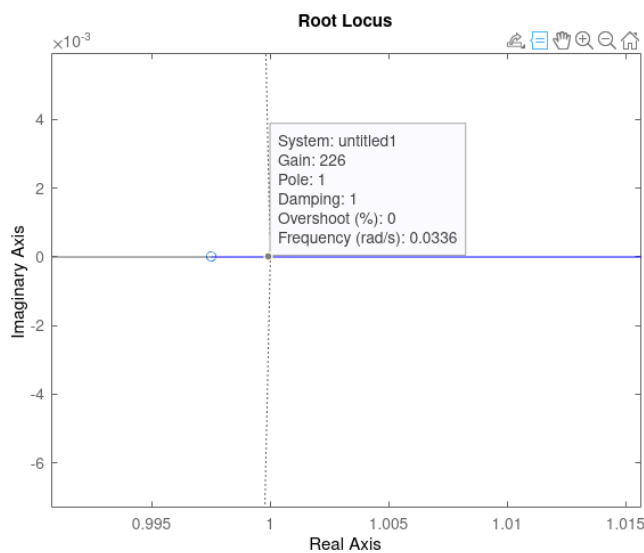


Figure 5.4: Detail of the root locus with K_p and K_d

The code used to carry out the analyses discussed up to this point in the section can be seen in

the Listing 8.1.

With these conclusions, the simulation of the system in Simulink is shown in the following two subsections, using the obtained gains in the z-domain to verify its performance.

5.2.1 Simulation of the plant without controller

Before simulating the system with the controller found using the root locus, the behaviour of the system found in Chapter 4 has been simulated to see that it really works as expected. To do this, a block diagram has been constructed in simulink, which can be seen in Figure 5.5.

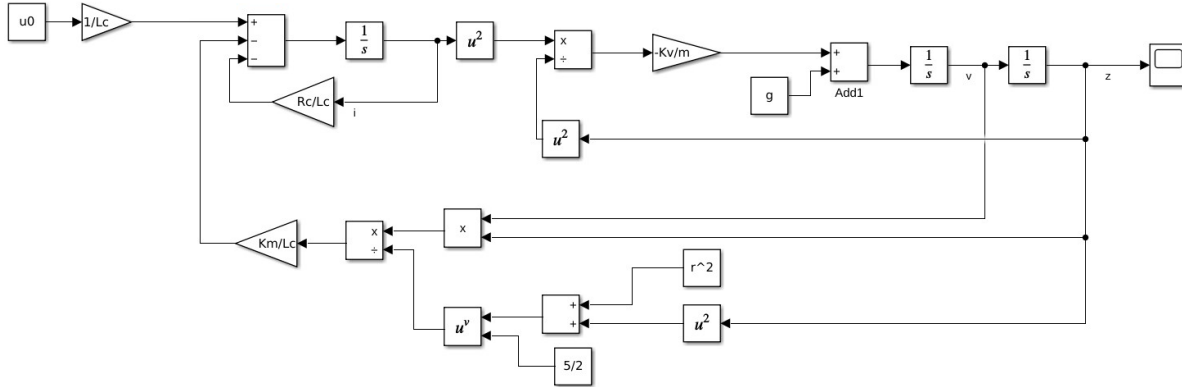


Figure 5.5: Open-loop system Simulink scheme

From there, taking into account that the equilibrium point found at z - from which the system has been linearised and the controller found - is 2.3 cm, the aim was to check that if the magnet is below this distance (for example, at 3 cm) it falls off and if, on the other hand, it is at 2 cm it sticks to the electromagnet. For this reason, the system has been simulated with these two initial conditions, thus obtaining the 5.6 and 5.7 figure, respectively, that prove that the system approximates the real behaviour of the levitator sufficiently well.

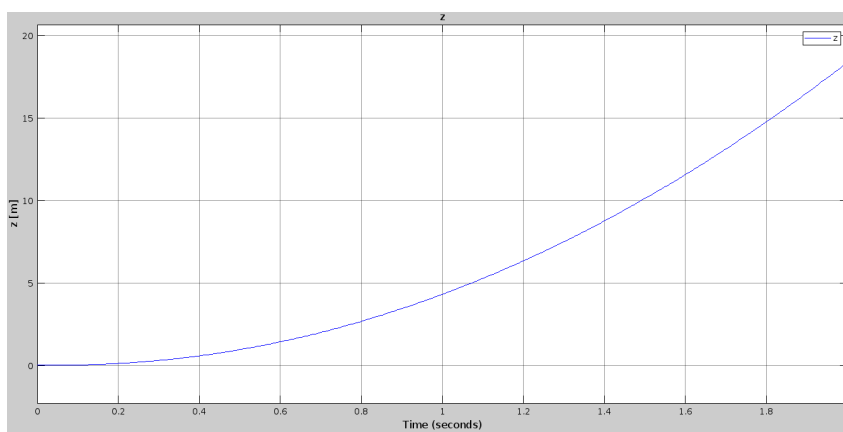


Figure 5.6: System output for z initial condition bigger than z^*

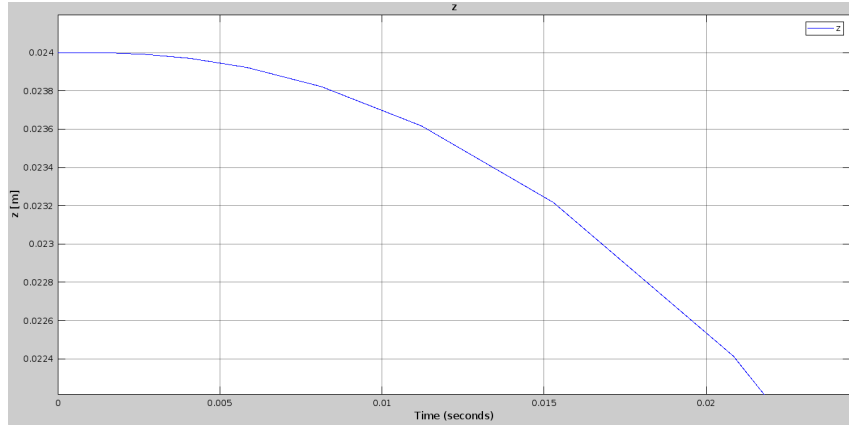


Figure 5.7: System output for z initial condition lower than z^*

5.2.2 Simulation of the closed loop system with PD

Once this verification of the system model has been carried out, the system is simulated in a closed loop and applying the PD controller previously found. For this purpose, starting from the previous simulation scheme, the modifications shown in figure 5.8 have been made.

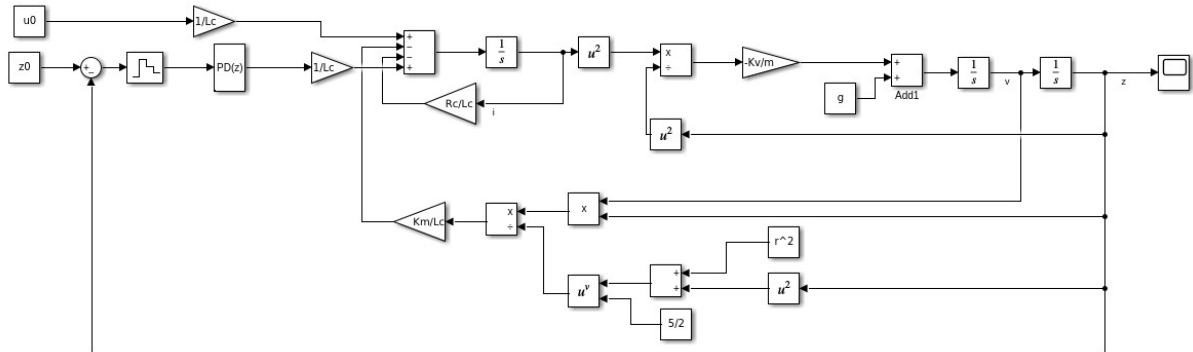


Figure 5.8: Closed loop system scheme to simulate the behavior with a PD controller

To run the simulation, it is obviously necessary to think about the initial conditions of the system. This system is highly non-linear so it is important that the initial z is already close enough to the equilibrium point. This is why a z_0 equal to 2.2 cm has been chosen. As expected, the output obtained (see Figure 5.9) indicates that the controller not only stabilises the system but also has no overshoot, the rise time is quite short and there is no damping or steady state error. It is worth mentioning that this is a simulation and, therefore, it is possible to achieve such a perfect result. However, in the next section it will be noted that it is not easy to find a controller with these characteristics in the real prototype.

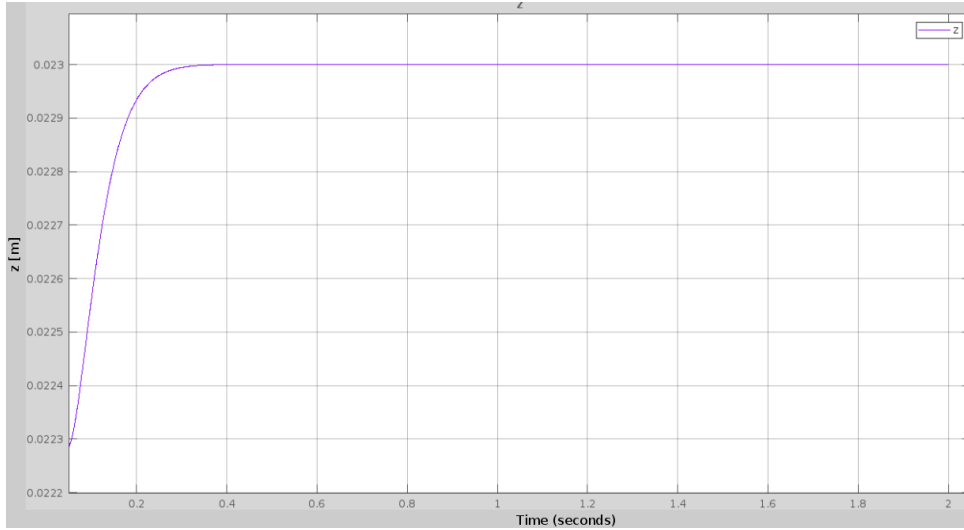


Figure 5.9: Response of the simulated system with a PD controller

5.3 Implementation of the controller and real-time system operation

As mentioned above, the real system is not so easy to handle. On the one hand, because the model of the system allows to simulate it with a certain resemblance to the real one, but it does not define exactly the real physical phenomena and the possible external disturbances. On the other hand, a new factor is added that did not exist in the simulation, the Hall effect sensor. In fact, the first thing that has given a lot of problems until we started to tune the PID constants was said sensor.

5.3.1 Sensor calibration

To be more precise, the fundamental problem has been that the chosen sensor measures the magnetic field strength on both sides of its housing. Therefore, it also measures the magnetic field generated by the electromagnet which, moreover, is varying since the state variable that we are modifying to find an equilibrium point is the current of the electromagnet, which is directly linked to the intensity of the magnetic field.

To mitigate the effect of the electromagnet on the sensor, two steps were taken. The first was not to place it exactly under the coil, but about 5mm away, thus reducing its effect on the measurement. The second and more important, was to calibrate the sensor in such a way that the effect of the electromagnet on the sensor could be cancelled out.

To perform this sensor calibration, the code shown in Listing 8.2 has been used, which basically increases in a loop the PWM applied to the electromagnet from -255 to 255 and measures the sensor measurement for each of these PWM values. With this procedure, the points plotted in Figure 5.10 are obtained. It can be seen that the magnetic field of the electromagnet varies linearly according to the PWM and three different slopes can be distinguished.

The linear regression has been carried out for each of these sections and, then, we have proceeded to see if with these regressions the effect of the sensor could be effectively cancelled out. For this purpose, the code available in the Listing 8.3 has been used.

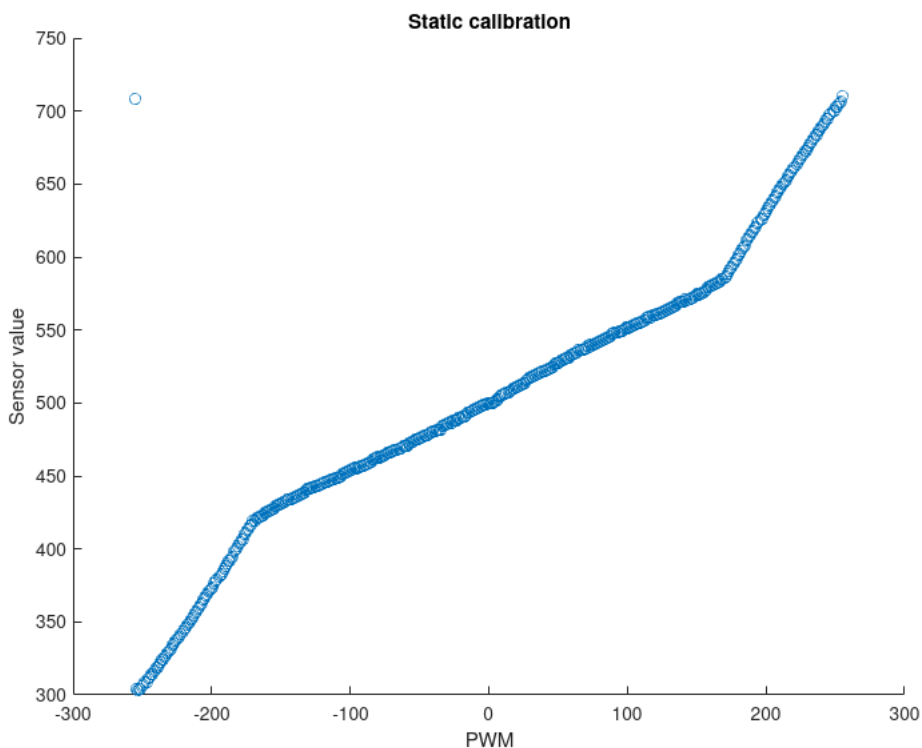


Figure 5.10: Sensor static calibration

This code, on the other hand, varies the PWM values between 220 and -220, maintaining one or the other for at least 100 loops before switching to the other value. This PWM value, depending on the section to which it corresponds according to graph 5.10, is applied to one of the 3 linear regressions and the value obtained from this is subtracted from that measured by the sensor. In this way, Figure 5.11 is obtained in which it can be seen how, despite the PWM changing between values of opposite sign, the effect of the electromagnet on the sensor measurements is cancelled out.

5.3.2 PID controller

To find the PID controller that stabilizes the real system, a systematic process that started with the simplest controller, a P-controller, was followed. Tuning the K_p parameter empirically, a certain value ($K_p=20$) for the proportional gain that stabilized the output of the system for a more or less 20 seconds was found. However, the resulting signal was very noisy and the steady-state error needed improvement(see Figure 5.12).

According to what has been said on the PID control theory and how each of the parts contributes to the whole controller, it can be recalled that the derivative term of a controller contributes positively to the controller's output by predicting the future error of the system based on its current rate of change. By taking the derivative of the error signal and adding it to the proportional term, the controller can anticipate any upcoming changes in the error signal and adjust the control input accordingly, helping to dampen the system's response and stabilize it by reducing oscillations caused by sudden changes in the system's input. With this in mind, the next step was to try to reduce the oscillations by adding the derivative part to the controller. This resulted in a more stable system (the sensor could levitate twice as long), but the noisy

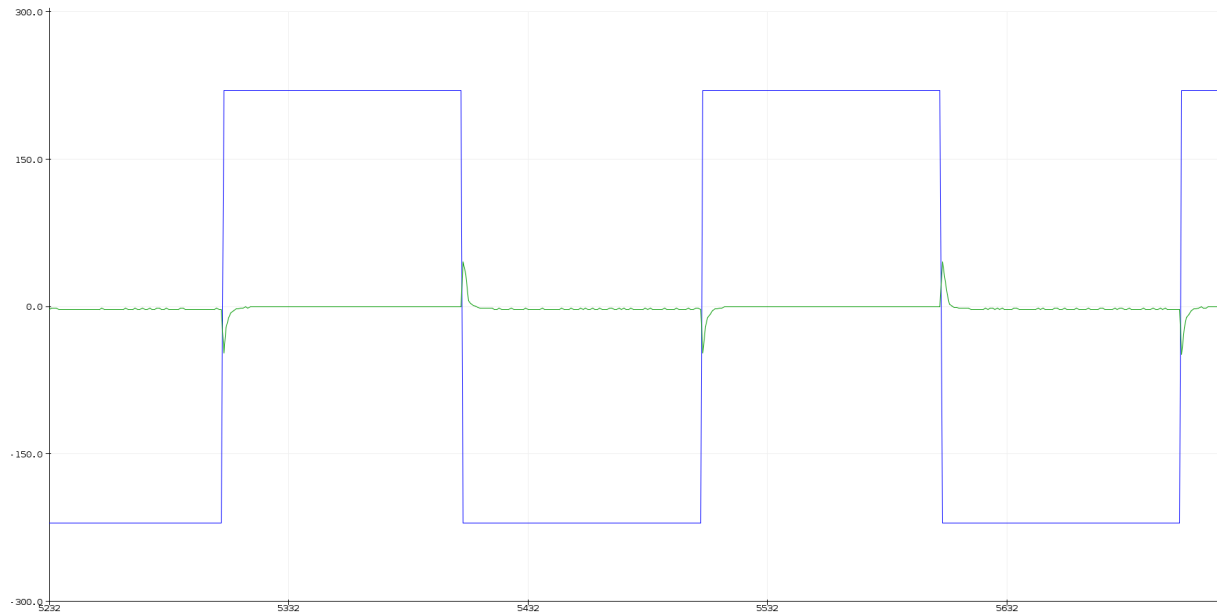


Figure 5.11: Cancelling out the coil effect on the Hall effect sensor dynamic

oscillations remained as can be seen in Figure 5.13.

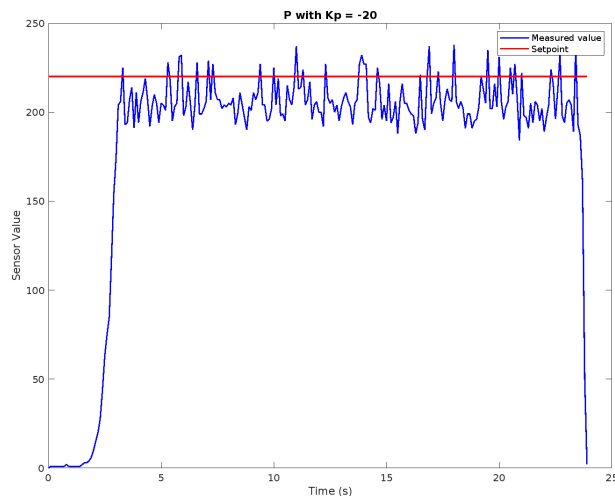


Figure 5.12: Response of the system with a P controller

Finally, taking into account that with this controller the steady state error can still be improved, it was decided to add the integral part which helps to improve this aspect. By adding this part, the other two parameters had to be touched in order to find a combination that would stabilise the system. This combination was: $K_p=-19.5$, $K_i=0.45$ and $K_d=0.0001$. It can be seen in Figure 5.14 that, indeed, this controller stabilises the response even more (the time that is maintained exceeds one minute now) and reduces the steady state error somewhat.

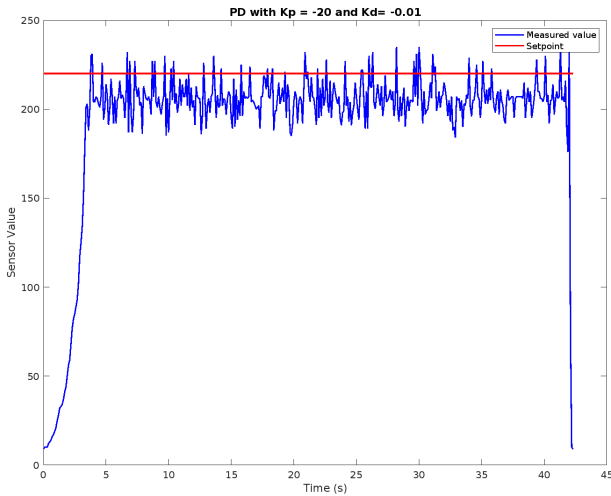


Figure 5.13: Response of the system with a PD controller

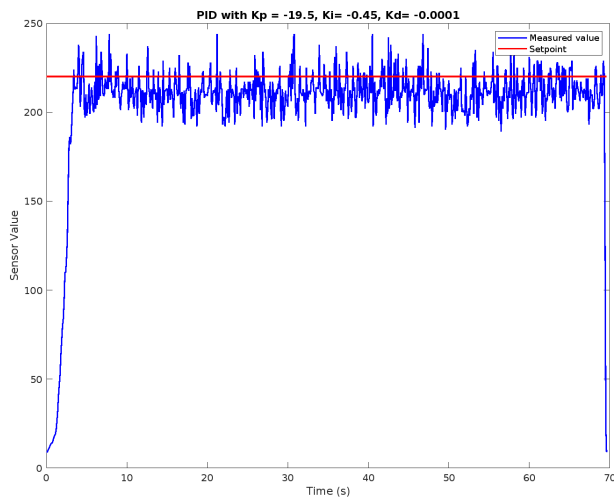


Figure 5.14: Response of the system with a PID controller

Up to this point, normal control has been carried out according to PID control theory using the code that can be seen in Listing 8.4. However, it can be observed that, even without the derivative part, the signal is already very noisy. As part of the experimentation of this project, it has been hypothesised that the sensor measurement for some reason returns the derivative of the measurement instead of the position itself and that is why these exaggerated oscillations occur.

Following this reasoning, it was thought that we could try to implement a PD similar to the one found in simulation and integrate the output of this PD to compensate the derivative of the sensor. With values of $K_p=-140$ and $K_d=-5$ and the new code that can be seen in Listing 8.5, a very good result was obtained in which the magnet could remain stable, with a decreased steady state error and much smoother oscillations (see Figure 5.15). Thus, the best controller found so far has been this one.

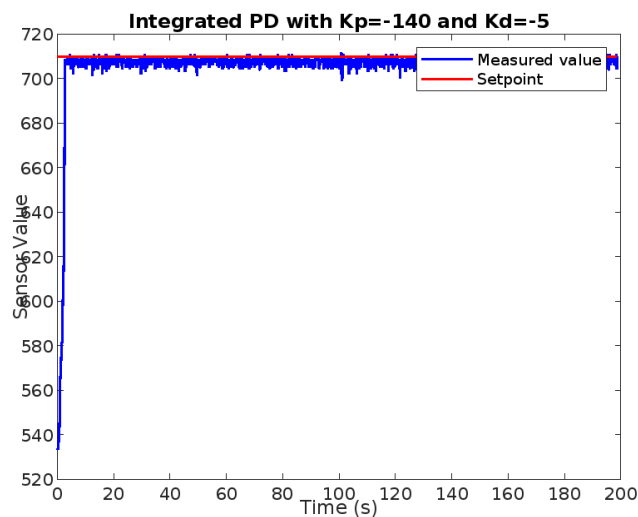


Figure 5.15: Response of the system with an integrated PD controller

Chapter 6

Project planning

This chapter includes a section where a Gantt chart has been constructed. The Gantt chart outlines the various tasks and milestones involved in the project, along with their estimated start and end dates. The purpose of this section is to provide a clear overview of the project timeline that helped ensure that the project stayed on track.

6.1 Gantt chart

To plan this project in the long term, a Gantt chart was constructed. This is a visual tool consisting of a series of horizontal bars representing the tasks to be carried out and their duration, organised on a time axis. This diagram made it possible to monitor the progress of the project.

To do this, the tasks and their durations were first defined:

Activity	Task description	Init date	End date
A1	Magnetic levitation research	November 7, 2022	November 30, 2022
A2	Component selection and structure design	December 1, 2022	December 28, 2022
A3	Magnetic levitator construction	December 14, 2022	January 14, 2023
A4	Sensor experimentation	January 14, 2023	January 21, 2023
A5	PID programming and tuning	January 22, 2023	February 28, 2023
A6	Application of advanced control techniques	March 1, 2023	March 31, 2023
A7	Drafting project report	March 15, 2023	April 22, 2023

From this data, the following graph was obtained:

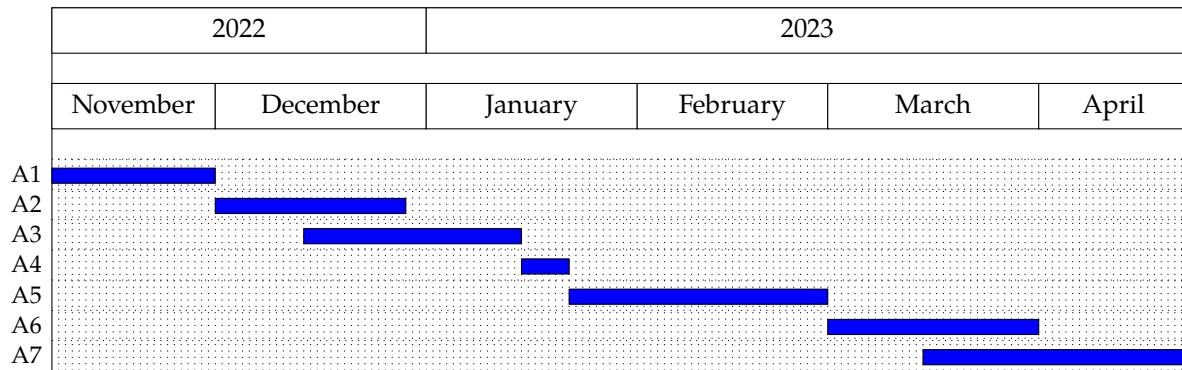


Figure 6.1: Gantt diagram of the project

Due to the strange behaviour of the sensor measurements, which as mentioned before it was concluded that instead of giving the measurement it returned the derivative of it, controlling through PID took very long, making it impossible to carry out the task of implementing more advanced and specific control methods for non-linear systems, such as sliding mode control.

Chapter 7

Project related costs

In any engineering project, managing costs is a critical aspect that can make the difference between success and failure. In particular for this project as one of the main objectives was to keep the cost of the prototype low. In this chapter, the costs associated with the design and implementation of the magnetic levitation prototype are analyzed in detail. Two main categories of costs are considered: the cost of the prototype itself and the cost of the electricity consumed during the project. The former includes the expenses related to the materials used to build the prototype. The latter involves the project energy consumption, which another expense to take into consideration. The aim of this chapter is to provide a comprehensive overview of the costs associated with the magnetic levitation project.

7.1 Cost of the prototype

In this section, the cost associated with the project of building and controlling a magnetic levitator prototype will be detailed. Mainly, the cost of the material used in the project will be broken down below, as the main purpose of the project was to construct an inexpensive prototype for education or entertainment purposes.

To begin with, here is a breakdown of material costs:

- **PLA box:** the printed piece should weigh at most about 100g. If 300-500 g of PLA filament costs about 10.00€, the piece costs 3.00€, approximately.
- **Arduino UNO Rev3:** 24.00€
- **Arduino Motor Shield Rev3:** 24.00€
- **12V 2A DC power supply:** 6.00€
- **Neodymium magnet:** 3.5€
- **Heschen electromagnet:** 10.00€
- **49E Hall effect sensor:** 10 sensors cost approximately 7.00€

- **Pack of Arduino jumper cables:** 4.00€

So the total spent on material to build a single prototype has been:

$$3.00\text{€} + 2 \cdot 24.00\text{€} + 6.00\text{€} + 3.50\text{€} + 10.00\text{€} + 7.00\text{€} + 4.00\text{€} = \mathbf{81.5\text{€}}$$

7.2 Electricity costs

In addition to the cost of the material, the other relevant cost would be electricity consumption. If in December 2022 the average cost of electricity in Spain was 0.335€/kWh [23], taking into account the total MWh calculated in Section 8.1, the cost of the project in electricity has been of:

$$0.335\text{€}/\text{kWh} \cdot 18.616\text{kWh} = \mathbf{6.23\text{€}}$$

Chapter 8

Project impact

This chapter aims to analyze the potential impact of the prototype of a magnetic levitation system on the environment and gender equality.

8.1 Environmental impact

The impact of the project on the environment is minimal considering the dimensions of the project and the prototype. However, it is still important to consider the potential environmental impacts of the materials and technologies that have been used.

One material that has a relatively high environmental impact is neodymium magnets, which are used in the project as the object to be levitated. The production process involved in extracting and refining rare earth metals, which are used to make these magnets, can generate significant environmental impacts, including air and water pollution, soil contamination and damage to ecosystems. Additionally, the production process can also consume significant amounts of energy and water. Disposal of neodymium magnets can also pose environmental risks, particularly if they are not properly recycled or disposed of at the end of their useful life.

The use of 3D printing materials, particularly plastics, can also have environmental impacts due to their production process, which requires the use of petroleum, a non-renewable resource that can generate significant greenhouse gas emissions. However, the use of 3D printing in the project has been limited and the impact is likely to be minimal.

Regarding the energy consumption, the Arduino and the motor shield were powered by a 12V power source. According to the Arduino specifications, the maximum consume would be of 50mA at 5V. Considering our supply voltage is 12V, the current would be approximately 120mA. Therefore, it consumes approximately 1.44 watts of power. The motor shield specifications indicate that the maximum current draw is 2 amperes, which, in turn, equates to a maximum power consumption of 24 watts.

Assuming that the project took the equivalent of 12 ECTS credits, which typically corresponds to 300 hours of work, the Arduino and motor shield were used for half that time, or 150 hours. Therefore, the total energy consumption for the Arduino and the motor shield can be estimated as follows:

$$E_{Arduino} = 1.44 \text{ watts} \times 150 \text{ hours} = 216 \text{ watt-hours}$$

$$E_{MotorShield} = 24 \text{ watts} \times 150 \text{ hours} = 3600 \text{ watt-hours}$$

In addition, the laptop was used throughout the entire project and its power consumption can be estimated at 50 watts. Assuming a project duration of 300 hours, the total energy consumption for the laptop can be estimated as follows:

$$E_{Laptop} = 50 \text{ watts} \times 300 \text{ hours} = 15000 \text{ watt-hours}$$

The total energy consumption for the project can be calculated by adding up the energy consumed by the Arduino, the motor shield and the laptop:

$$E_{total} = E_{Arduino} + E_{MotorShield} + E_{Laptop} = 18616 \text{ watt-hours}$$

For comparison, a typical washing machine uses about 1500 watts per hour, so the total energy consumed by the project is equivalent to approximately 12 hours of washing machine operation. Therefore, it can be concluded that the environmental impact of this project is minimal and the energy consumption is negligible when compared to the daily energy consumption of common household appliances.

8.2 Impact on gender equality

Another aspect that can be studied in any engineering project is the potential impact of gender. However, it is difficult to identify specific gender-related impacts of this particular project, as technical knowledge and skills are the primary factors required for its successful implementation.

While the impact of gender on the project may not be immediately apparent, the mere fact that a woman lead this project demonstrates that engineering is not limited to men and serves as an important reminder of the need for diversity in STEM fields.

Conclusions

The project aimed to create a low-cost magnetic levitation prototype for educational purposes to learn about system control. The objective was achieved by developing a functional prototype with a PID control system implemented on an Arduino board at an affordable price. However, unexpected behavior from the sensor led to more time being spent on developing the PID control for the levitator, which prevented the implementation of more advanced control systems such as sliding mode control.

Future development could be improved by using a more powerful microcontroller to enable the implementation of more advanced control systems beyond PID, as the current Arduino board has limitations due to its limited computing power and speed. This would allow for exploration and implementation of e.g. nonlinear control strategies.

In conclusion, although the project encountered some setbacks during development, a working model that is affordable was produced and can be used to teach and learn about control systems. Upgrading to a more powerful microcontroller could unlock the potential to implement more advanced control systems and is recommended as a next step for future development.

Acknowledgements

I would like to express my deep gratitude to Manel Velasco, my project supervisor, for his guidance and support throughout this endeavor. His expertise, patience and encouragement have been invaluable in helping me achieve my goals. I am grateful for the opportunity to work under his mentorship and learn from his wealth of knowledge.

I would like to express my sincere gratitude to my friends at CL for their amazing support and encouragement during this challenging project. In particular, I am thankful to Gerard for lending me his milling machine and 3D printer, which played an important role in constructing the prototype. Their generosity and support have been priceless and I am grateful for their contributions to the successful completion of this project.

Lastly, I want to thank my parents for their constant love and emotional support. Their belief in me has been the driving force behind my success and I am deeply grateful for everything they have done for me. Their unwavering support has given me the strength and determination to achieve the project goals.

Bibliography

- [1] MIKEROV, A.G., 2014. From history of Electrical Engineering III: Electromagnetism discovery and its fundamental laws in the first half of 19-th century. *Proceedings of the 2014 IEEE NW Russia Young Researchers in Electrical and Electronic Engineering Conference*. S.l.: IEEE, pp. 1-7. ISBN 9781479925933. DOI 10.1109/ElConRusNW.2014.6839186.
Consulted on: November 2022
- [2] MRTOLO, M., Araneo, R., 2019. A Brief History of Electromagnetism [History]. *IEEE industry applications magazine*, vol. 25, no. 2, pp. 7-11. ISSN 1077-2618. DOI 10.1109/MIAS.2018.2884753.
Consulted on: November 2022
- [3] KIPNIS, N., 2005. Chance in Science: The Discovery of Electromagnetism by H.C. Oersted. *Science & education*, vol. 14, no. 1, pp. 1-28. ISSN 0926-7220. DOI 10.1007/s11191-004-3286-0.
Consulted on: November 2022
- [4] HAN, H.-S., Kim, D.-S., 2016. *Magnetic Levitation Maglev Technology and Applications*. 1st ed. 2016. Dordrecht: Springer Netherlands. ISBN 94-017-7524-9.
Consulted on: November 2022
- [5] LIVINGSTON, J.D., 2011. *Rising force the magic of magnetic levitation*. Cambridge, Mass: Harvard University Press. ISBN 0-674-06109-8.
Consulted on: November 2022
- [6] KHAMESEE, M.B., Kato, N., Nomura, Y. and Nakamura, T., 2002. Design and control of a microrobotic system using magnetic levitation. *IEEE/ASME transactions on mechatronics*, vol. 7, no. 1, pp. 1-14. ISSN 1083-4435. DOI 10.1109/3516.990882.
Consulted on: November 2022
- [7] ZHANG, D., Wei, B., 2016. Magnetically Driven Microrobotics for Micromanipulation and Biomedical Applications. *Advanced Mechatronics and MEMS Devices II*. Switzerland: Springer International Publishing AG, pp. 613-635. ISBN 3319321781.
Consulted on: November 2022
- [8] DABBAGH, S.R., Alseed, M.M., Saadat, M., Sitti, M., Tasoglu, S., 2022. Biomedical Applications of Magnetic Levitation. *Advanced NanoBiomed Research (Online)*, vol. 2, no. 3, pp. 2100103-n/a. ISSN 2699-9307. DOI 10.1002/anbr.202100103.
Consulted on: December 2022

- [9] Kaman Sensors. Magnetic Bearings. [online] Available at: <https://www.kamansensors.com/industry/magnetic-bearings>
Consulted on: April 2023
- [10] ASATO, K., Teruya, K., Nagado, T., Tamaki, S., 2017. Development of Magnetic Levitation System for Science and Technology Education: Magnetic Levitation Control by Using a Hall Element Displacement Sensor with Neural Network. *Electrical engineering in Japan*, vol. 200, no. 2, pp. 51-60. ISSN 0424-7760. DOI 10.1002/eej.22975.
Consulted on: November 2022
- [11] BERKELMAN, P., Lu, Y.-S. (2020). Long Range Six Degree-of-Freedom Magnetic Levitation Using Low Cost Sensing and Control. *Journal of Robotics and Mechatronics*, 32(5), 683-695. <https://doi.org/10.20965/jrm.2020.p0683>
Consulted on: November 2022
- [12] MOHAMAD, N.R.B. ET AL., 2012. Electromagnetic levitator. *2012 International Conference on Computer and Communication Engineering (ICCCE)*. S.l.: IEEE, pp. 319-324. ISBN 1467304786. DOI 10.1109/ICCCE.2012.6271204.
Consulted on: November 2022
- [13] SILVA, B.E., Barbosa, R.S., 2021. Experiments with Neural Networks in the Identification and Control of a Magnetic Levitation System Using a Low-Cost Platform. *Applied sciences*, vol. 11, no. 6, pp. 2535-. ISSN 2076-3417. DOI 10.3390/app11062535.
Consulted on: November 2022
- [14] About Arduino. *Arduino - Home* [online]. Available at: <https://www.arduino.cc/en/about>
Consulted on: March 2023
- [15] Arduino Uno Rev3. *Arduino Official Store* [online]. [sin fecha] Available at: <https://store.arduino.cc/products/arduino-uno-rev3>
Consulted on: March 2023
- [16] 49E Linear Hall-Effect Sensor. *MikroElectron online electronics store* [online]. Available at: <https://mikroelectron.com/Product/49E-Linear-Hall-Effect-Sensor>
Consulted on: March 2023
- [17] Heschen Electromagnet Magnet Solenoid. *Heschen* [online]. Available at: <https://heschen.com/products/b078ksyn1s>
Consulted on: April 2023
- [18] Arduino Motor Shield Rev3. *Arduino Official Store* [online]. Available at: <https://store.arduino.cc/products/arduino-motor-shield-rev3>
Consulted on: March 2023
- [19] Basics of PWM (Pulse Width Modulation), Arduino Documentation. *Arduino Docs | Arduino Documentation*. Available at: <https://docs.arduino.cc/learn/microcontrollers/analog-output>
Consulted on: April 2023

- [20] LAFUENTE LARRAÑAGA, J. S.. *Design and Development of a Digitally Controlled Magnetic Levitation System*. Master thesis. Universidad del País Vasco, 2019. Available at: <http://hdl.handle.net/10810/36694>
Consulted on: February 2023
- [21] KINGMAN, R., Rowland, S.C., Popescu, S., 2002. An experimental observation of Faraday's law of induction. *American Journal of Physics*, 70, 595-598. <https://doi.org/10.1119/1.1405504>
Consulted on: February 2023
- [22] RAMOS LARA, R.R., 2007. TEMA 6 Sistemas Digitales de Control en Tiempo Discreto. *Universitat Politècnica de Catalunya*. Available at: <https://upcommons.upc.edu/bitstream/handle/2117/6123/TEMA6.pdf>
Consulted on: March 2023
- [23] España - Precios de la electricidad de los hogares 2022. *Expansion* [online]. Available at: <https://datosmacro.expansion.com/energia-y-medio-ambiente/electricidad-precio-hogares/espana>
Consulted on: March 2023

Annexes

```
1 %% Initialization:  
2 clear all; close all; clc;  
3 %% Setup of the magnetic levitation system parameters  
4 % Coil Inductance (H)  
5 Lc = 0.056;  
6 % Coil Resistance (Ohm)  
7 Rc = 38;  
8 % Coil radius (m)  
9 r = 0.0125;  
10 % Coil length (m)  
11 l = 0.02;  
12 % Area of the coil facing the levitating object  
13 A = pi*r^2;  
14 % Permeability of free space  
15 mu0 = 4*pi*1e-7;  
16 % Number of turns of the coil  
17 N= sqrt(Lc*l/(mu0*A));  
18  
19 % Magnet mass (kg)  
20 m = 0.010;  
21 % Gravitational Earth constant (m/s^2)  
22 g = 9.81;  
23  
24 Km = 3/2*mu0*m*N*r^2;  
25  
26 %% Equilibrium point  
27 u0 = 7.1;  
28 z0 = 0.023;  
29 v0 = 0.0;  
30 i0 = 0.132;  
31  
32 syms Kv  
33 eqn = g-(Kv/m)*(i0^2/z0^2) == 0;  
34 [A,B] = equationsToMatrix([eqn], [Kv])  
35 X = linsolve(A,B);  
36 Kv = double(X)  
37  
38
```

```

39 %% TRANSFERENCE FUNCTION AND DISCRETIZATION
40
41 A21=2*Kv*i0^2/(m*z0^3);
42 A23=-2*(Kv/m)*(i0/(z0^2));
43 A32=-Km*z0/(Lc*(r^2+z0^2)^(5/2));
44 A33=-Rc/Lc;
45
46 A=[0,1,0;A21,0,A23;0,A32,A33];
47 B=[0;0;(1/Lc)];
48 C=[1,0,0];
49 D=[0];
50 sys = ss(A, B, C, D);
51
52 [num,den]=ss2tf(A,B,C,D);
53 Gs=tf(num,den);
54
55 Ts = 0.0025;
56 Gz = c2d(Gs,Ts);
57
58 Kp = -220;
59 Ki = 0;
60 Kd = -2.5;
61 Cz = pid(Kp, 0, Kd, 0, Ts);
62
63 % Root locus of the open-loop tranfer function
64 rlocus(Gz*Cz);
65
66 % Closed loop TF
67 G_cl = feedback(Gz*Cz,1);
68
69 % Poles of the controlled system
70 poles = pole(G_cl)

```

Listing 8.1: Matlab code to find Root Locus and closed loop poles of the system

```

1 int dir=0;
2 int pwm = -256;
3 volatile float hallValue;
4 int PWM_pin = 3; // set the PWM input pin for channel A
5 int dir_pin=12;
6 const int hallPin = A4;
7 void setup() {
8     pinMode(PWM_pin, OUTPUT); // initialize the PWM pin
9     pinMode(dir_pin,OUTPUT);
10    attachInterrupt(digitalPinToInterrupt(PWM_pin), pwmInterrupt,
11                     FALLING);
12
13    // rest of setup code
14    Serial.begin(57600);

```

```

14  while (!Serial);           // wait for the serial monitor to open
15 }
16
17 void pwmInterrupt() {
18     // This function is called when the PWM cycle is completed
19     hallValue = analogRead(hallPin);
20 }
21
22 void loop() {
23     pwm=pwm+1;
24     if (pwm==256)
25     {
26         Serial.println("-----");
27         pwm=-255;
28     }
29     if(pwm>=0){dir=0;}
30     if(pwm<0){dir=1;}
31     int pwm_a=abs(pwm);
32
33     digitalWrite(12,dir);
34     analogWrite(PWM_pin, pwm_a);
35     delay(10);
36
37     // Print the values to the serial monitor
38     Serial.print(pwm);
39     Serial.print(" ; ");
40     Serial.println(hallValue);
41 }
```

Listing 8.2: Arduino code to perform the static calibration of the sensor

```

1 int dir=0;
2 int pwm = -256;
3 volatile float hallValue;
4 int PWM_pin = 3; // set the PWM input pin for channel A
5 int dir_pin=12;
6 const int hallPin = A4;
7 float prev_val=0;
8 int counter=0;
9
10 void setup() {
11     pinMode(PWM_pin, OUTPUT); // initialize the PWM pin
12     pinMode(dir_pin,OUTPUT);
13     attachInterrupt(digitalPinToInterrupt(PWM_pin), pwmInterrupt,
14                     FALLING);
15
16     // rest of setup code
17     Serial.begin(57600);
18     while (!Serial); // wait for the serial monitor to open
```



```

18 }
19
20 void pwmInterrupt() {
21 // // This function is called when the PWM cycle is completed
22 hallValue = analogRead(hallPin);
23 }
24
25 void loop() {
26 counter=counter+1;
27 if (counter==100){pwm=220; }
28 if (counter==200){pwm=-220; counter=0; }
29 if (pwm>=0) {dir=0; }
30 if (pwm<0) {dir=1; }

31 float addi=0.0751*pwm+506.5192; // Regression for intermediate pwm
32     values
33 float addi_small=0.1961*pwm+527.0108; // Regression for small pwm
34     values
35 float addi_large=0.2013*pwm+485.3296; // Regression for large pwm
36     values

37 if(pwm>169) {
38     addi=addi_large;
39 }
40 if(pwm<-171) {
41     addi=addi_small;
42 }
43 int pwm_a=abs(pwm);

44 digitalWrite(12,dir);
45 analogWrite(PWM_pin, pwm_a);
46 prev_val=hallValue-addi;

47 // Print the values to the serial monitor
48 Serial.print(pwm);
49 Serial.print(" ; ");
50 Serial.println(prev_val);
51 delay(1);
52 }

```

Listing 8.3: Arduino code to check the electromagnet effect is cancelled out

```

1 int anaPin = 4;    // Arduino Analogic Pin 4
2 int pwmPin = 3;
3 int dirPin = 12;
4 //
5 float sensorVal = 0.0;    // Analogic Value
6 int measured_value = 0; // Sensor value without electromagnet effect
7 int dir = 0;

```

```
8 //  
9 int setpoint = 220; // Levitation Value  
10 //  
11 float timeVal = 0; // timeVal Value  
12 //-----|  
13 // PID Values  
14 float output = 0;  
15 float integral = 0;  
16 float derivative = 0;  
17 float error = 0;  
18 float previous_error = 0;  
19 float dt = 0.0025;  
20 float Ki = -0.45;  
21 float Kd = -0.00001;  
22 float Kp = -19.5;  
23 //-----|  
24 // Anti-windup variables  
25 double integralTermMax = 264;  
26 double integralTermMin = -264;  
27 //-----|  
28 void setup()  
29 {  
30     // Levitator initialization Begin;  
31     Serial.begin(57600);  
32  
33     pinMode(pwmPin, OUTPUT); // initialize the PWM pin  
34  
35     pinMode(dirPin, OUTPUT);  
36  
37     timeVal = millis();  
38     // Levitator initialization End;  
39     Serial.println("Started.");  
40 }  
41 //-----|  
42  
43  
44 void loop() // PID  
45 {  
46     sensorVal = analogRead(anaPin);  
47  
48     float addi=0.0751*output+506.5192;  
49     float addi_p=0.1961*output+527.0108;  
50     float addi_g=0.2013*output+485.3296;  
51  
52     if(output>169){  
53         addi=addi_g;  
54     }  
55  
56     // PID calculations
```



```

57 measured_value = int(sensorVal - addi);
58 error = measured_value - setpoint;
59 integral = integral + error * dt;
60 // ANTI WINDUP EFFECT
61 if (integral > integralTermMax) {
62     integral = integralTermMax;
63 } else if (integral < integralTermMin) {
64     integral = integralTermMin;
65 }
66 derivative = (error - previous_error) / dt;
67 output = (Kp * error) + (Ki * integral) + (Kd * derivative);
68 previous_error = error;
69
70 // Saturation;
71 if (output < 0) output=0;
72 if (output > 255) output=255;
73
74 int pwm=abs(output);
75
76 digitalWrite(dirPin,dir);
77 analogWrite(pwmPin, pwm);
78
79 // Show log values for debug;
80 if((millis()-timeVal) > 100)
81 {
82     print_logs();
83     timeVal = millis();
84 }
85 }
86 //-----|
87 void print_logs()
88 {
89     // Show the Hall Sensor Value;
90     Serial.print(measured_value);
91     Serial.print(";");
92     Serial.println(setpoint);
93 }
```

Listing 8.4: Arduino code used to tune PID

```

1 int anaPin = 4;    // Arduino Analogic Pin 4
2 int pwmPin = 3;
3 //
4 int sensorVal = 0;    // Hall sensor measurement
5 int output_int = 0;    // Final PWM sent to electromagnet
6 //
7 int setpoint = 710;
8 //
9 float timeVal = 0; // Time Value
```

```
10 //-----|  
11 // PID Values  
12 float output = 0;  
13 float integral = 0;  
14 float derivative = 0;  
15 float error = 0;  
16 float previous_error = 0;  
17 float dt = 0.0025;  
18 float Kp = -140.0;  
19 float Ki = -0.0;  
20 float Kd = -5.0; // 10  
21 //-----|  
22 // Anti-windup variables  
23 int bias = 200;  
24 double integralTermMax = 264;  
25 double integralTermMin = -264;  
26 //-----|  
27 void setup()  
28 {  
29     // Levitator initialization Begin;  
30     Serial.begin(57600);  
31     Serial.println("Starting...");  
32     //  
33     timeVal = millis();  
34     setpoint = levVal;  
35     // Levitator initialization End;  
36     Serial.println("Started.");  
37 }  
38 //-----|  
39 void loop()  
40 {  
41     // Hall Sensor Read (Magnetic Field Intensity);  
42     sensorVal = analogRead(anaPin);  
43     // PID calculations  
44     error = setpoint - measured_value;  
45     integral = integral + error * dt;  
46     if (integral > integralTermMax) {  
47         integral = integralTermMax;  
48     } else if (integral < integralTermMin) {  
49         integral = integralTermMin;  
50     }  
51     derivative = (error - previous_error) / dt;  
52     output = (-Kp * error) + (-Ki * integral) + (-Kd * derivative);  
53     previous_error = error;  
54     // Integrated PD  
55     output_int += output;  
56     // Apply saturation in the PWM limits;  
57     if (output_int < 0) output_int=0;  
58     if (output_int > 255) output_int=255;
```

```
59     analogWrite(pwmPin, output_int);
60
61 // Print log values
62 if((millis()-timeVal) > 100)
63 {
64     print_logs();
65     timeVal = millis();
66 }
67 }
68 }
69 //-----|
70 void print_logs()
71 {
72     Serial.print(sensorVal);
73     Serial.print(";");
74     Serial.println(setpoint);
75 }
76 //=====|
```

Listing 8.5: Arduino code for the integrated PD